Characterizing current and predicting future variability of organic matter in runoff from upland peat catchments

A thesis submitted to the University of Manchester for the degree of Master of Environmental, Atmospheric and Earth Sciences by Research in Faculty of Science & Engineering

2019

Phillip A. Agredazywczuk (9699128)

School of Natural Sciences, Department of Materials

Contents

Wordcount: 19,103

Table of Figures

List of Tables

Abstract

Peatlands are a global carbon store that is predicted to be adversely affected by global warming, in which the amount of organic carbon they release may increase. Indirect carbon dioxide fluxes from run-off are likely to be larger and harder to quantify than direct fluxes. This study simulated future climate conditions by monitoring a damaged (eroded) catchment paired with an intact (vegetated) catchment. Bulk carbon fluxes for the vegetated and eroded catchment were; 17.57 t km^{-2} yr^{-1} and 108.30 t km^{-2} yr^{-1} calculated via interpolation, and 31.57 t km^{-2} yr^{-1} and 65.48 t km^{-2} yr^{-1} calculated via rating relationships. Attempts were made to identify differences in hydrology between the vegetated and eroded catchments, particularly before and after remediation of the eroded catchment, attempted in 2007. The pH and hydrogen ion concentration did not differ between the two catchments. Prior to restoration, time to peak and run-off coefficients appeared to be unaltered; although, there is a suggestion that conditions may have improved at the eroded catchment in 2019. There were also differences between organic carbon fluxes subdivided into sub-micron size classes (<1.6>0.2 µm, <0.2 µm>50 kDa, <50>10 kDa and <10>3 kDa). Fluxes at the vegetated catchment were larger than the eroded; 48.64 43 t km^{-2} yr^{-1} and 34.92 43 t km^{-2} yr^{-1}. The distrubution of the flux remained relatively similar, the two smallest fractions remaining dominant. Carbon dioxide production from samples of organic carbon classifications showed smaller sizes to have greater lability. Inorganic carbon, only dissolved carbon dioxide considered, was consistently supersaturated on average by 545 ppm at the vegetated catchment and 214 ppm at the eroded. Carbon dioxide concentrations decreased at both sites during an event. In a global warming scenario where peat is likely to become similar to the eroded catchment; the organic carbon flux is likely to increase and the sub-micron flux will potentially be smaller, but the distribution of this will remain the same.

Declaration

I declare that no portion of the work referred to in the dissertation has been submitted in support of an application for another degree or qualification of this or any other university or other institute of learning.

Copyright statement

i. The author of this thesis (including any appendices and/or schedules to this thesis) owns certain copyright or related rights in it (the “Copyright”) and s/he has given The University of Manchester certain rights to use such Copyright, including for administrative purposes.

ii. Copies of this thesis, either in full or in extracts and whether in hard or electronic copy, may be made only in accordance with the Copyright, Designs and Patents Act 1988 (as amended) and regulations issued under it or, where appropriate, in accordance Presentation of Theses Policy You are required to submit your thesis electronically Page 11 of 25 with licensing agreements which the University has from time to time. This page must form part of any such copies made.

iii. The ownership of certain Copyright, patents, designs, trademarks and other intellectual property (the “Intellectual Property”) and any reproductions of copyright works in the thesis, for example graphs and tables (“Reproductions”), which may be described in this thesis, may not be owned by the author and may be owned by third parties. Such Intellectual Property and Reproductions cannot and must not be made available for use without the prior written permission of the owner(s) of the relevant Intellectual Property and/or Reproductions.

iv. Further information on the conditions under which disclosure, publication and commercialisation of this thesis, the Copyright and any Intellectual Property and/or Reproductions described in it may take place is available in the University IP Policy (see http://documents.manchester.ac.uk/DocuInfo.aspx?DocID=2442 0), in any relevant Thesis restriction declarations deposited in the University Library, The University Library’s regulations (see http://www.library.manchester.ac.uk/about/regulations/) and in The University’s policy on Presentation of Theses

Acknowledgements

Firstly, I would like to thank Dr. Steve Boult for all his support throughout my university career. I do not think without his guidance and teaching I would have become the student I am today, and hopefully researcher in the future.

Secondly, I would like to thank Felipe Rojas Parra, Tianming Wang, Wei Li for their helping hand in the lab and generally improving my experience during my MSc.

Lastly, I would like thank my mother for reading my consistent drafts and re-drafts.

1.0 Introduction

Peatlands only cover 2-3% of the Earth's surface, yet are considered a long term global carbon store with estimations between 270–370 Tg (teragrams) of global terrestrial carbon (Charman, 2002; Limpens, et al., 2008; Parry, et al., 2014). Peatland draining catchments naturally receive stored organic carbon through surface run-off (Parry, et al., 2014). A number of carbon forms can be present in the subsequent solution; (i) particulate organic carbon (POC), (ii) dissolved organic/inorganic carbon (DOC/DIC) and (iii) gaseous carbon i.e. free carbon dioxide (CO_2) (Worrall, et al., 2004; Evans, et al., 2006; Dinsmore, et al., 2010). In the current climatic situation, there is a potential for drastic change in rainfall, temperature patterns and intensity of droughts. It is predicted that these changes will cause similar erosional damage to peatlands caused by live-stock grazing, burning or artificial drainage (Holden, et al., 2007; Fenner & Freeman, 2011; Ise, et al., 2011). All can lead to enhancing the magnitude of carbon released into neighbouring fluvial systems, modifying these traditional stores to potential sources of carbon and act as a positive feedback to global warming (Weltzin, et al., 2003; Evans, et al., 2006).

Fluvial organic carbon has been observed to be a major loss pathway in peatlands (e.g. Billett, et al., 2004; Dawson, et al., 2004; Limpens, et al., 2008; Pawson, et al., 2008). A variety of biological or photochemical degradation processes can act on organic carbon in stream (e.g. Miller & Zepp, 1995; Amon & Benner, 1996; Montagnes, et al., 2008; Lapierre, et al., 2013; Moody, et al., 2013; Lapierre & Giorgio, 2014; Jones, et al., 2016; Pickard, et al., 2017; Stimson, et al., 2017; Brown, et al., 2018). The main product of the degradation reaction is carbon dioxide. Thus, fluvial organic carbon fluxes are a large potential source of carbon dioxide to the atmosphere.

Quantifying the potential flux is made difficult based on organic carbons highly complex and heterogeneous nature. It can be defined in to three major chemical groups; humic acids (HA), fulvic acids (FA) and humins. Although hetrogenity is not only chemical but also physical, with

an infinite range of particle size distrubutions (Nebbioso & Piccolo, 2013; Sillanpää, et al., 2014). The proportion of organic carbon that is reactive is determined by its lability which is regulated by composition, age and size (e.g. Palmer, et al., 2001; Billett, et al., 2007; Mann, et al., 2012; Stimson, et al., 2017; Stimson, et al., 2017). It is essential then to determine the reactivity of organic carbon in the hydrological environment.

There have been far less studies on the fluvial inorganic carbon in these areas (e.g. Hope, et al., 2001; Palmer, et al., 2001; Billett, et al., 2004; Dawson, et al., 2004; Hope, et al., 2004; Billett, et al., 2007). Previously carbon dioxide concentrations in fluvial systems were thought to be analogous with atmospheric concentrations (Weiss, 1974). However, numerous studies have shown that supersaturation of carbon dioxide, in respect to the atmosphere is common in many fluvial environments (e.g. Hope, et al., 2004; Mayorga, et al., 2005; Billett & Moore, 2008; Dinsmore & Billett, 2008; Johnson, et al., 2008; Dinsmore, et al., 2010; Johnson, et al., 2010). Supersaturation can lead to evasion of carbon dioxide from the water surface, evasion rates are controlled by a number of factors i.e. temperature, pH or flow hydraulics (e.g. Billett, et al., 2004; Dawson, et al., 2004; Hope, et al., 2004; Billett & Moore, 2008; Dinsmore, et al., 2009; Dinsmore, et al., 2013). Flow hydraulics of a stream have been suggested as a significant control of carbon dioxide evasion, flow intensity and partial pressure of carbon dioxide considered dominant (Long, et al., 2015). First-order streams commonly have high flow intensities and heavily mixed waters, thus are considered “hotspots” of carbon dioxide release. A number of first-order streams are located in upland peat environments (Butman & Raymond, 2011; Wallin, et al., 2012; Stimson, et al., 2017). The result is the degassing of carbon dioxide from the surface of streams and rivers directly linking peatlands to the atmosphere. As a potentially large direct carbon dioxide flux, it is necessary to understand and predict inorganic carbon concentrations in these areas.

The aims of this study is characterising current and predicting the future variability of organic carbon in run-off from upland peat catchments. A major difficulty of achieving this aim arises in the prediction of the future, as conditions are yet to occur. Thus, there is a requirement for

the study site to provide a suitable simulation of the future. The Peak District, UK provides a mosaic of eroded and intact peatlands induced by previous anthropogenic activities over the last century (Evans, et al., 2006). The Crowden Great Brook provides vegetated and eroded sub-catchments within a similar area which enables evaluation to the extent that climate change will have on these areas.

The requirement to predict an accurate organic carbon flux for a system is crucial. The highly variable spatial and temporal nature of these systems can impede estimations. High discharges are usually a low percentage of the time and it is known that this is when most material is moving (Grieve, 1990; Evans, et al., 2006; Pawson, et al., 2008; Pawson, et al., 2012). Without sampling regimes that capture these rapid spatial-temporal changes, an underestimation of the flux is likely to occur. Many sampling regimes can be accused of being too short in terms of temporal scale; not accounting for the potential spatial-temporal variabilities of a longer time-scale in catchments. Automated-samplers have been applied in a number of studies (Evans, et al., 2006; Stimson, et al., 2017; Stimson, et al., 2017). The apparatus can be pre-programmed to required sampling frequencies. A viable solution to provide higher spatial-temporal resolution but they can only provide this resolution for a finite period as they have a limited storage capacity. Thus, there is a requirement to estimate the flux on a longer temporal scale.

A variety of methods can be employed to estimate carbon fluxes such as interpolation or extrapolation techniques i.e. rating relationships (e.g. Worral, et al., 2003; Hope, et al., 2001; Dawson, et al., 2004; Evans, et al., 2006; Pawson, et al., 2008; Pawson, et al., 2012). Previous work has indicated that these methods can lead to underestimations or overestimations, attributed to the resolution of sample collection (Walling & Webb, 1981). Errors can be reduced through the minimisation of time intervals between discharge and corresponding organic concentrations in the two methods, and increasing the number of samples for the rating method (Evans, et al., 2006; Pawson, et al., 2008). Rating methods inclusion of flow weighting of carbon concentrations can also improve accuracy. Walling & Webb (1981) observed a

discrepancy in flux calculation when different temporal scales were used, rating relationships calculated using daily discharges were observed to be lower than estimates that utilised hourly discharges. Rating relationships can be affected by the spatial-temporal distribution of organic carbon concentrations over the course of an event. When samples are collected, a time series of the event is captured, discharge and concentration relationships are not likely to be perfect linear relationships. For this reason, rating relationships will be split into *event* ratings, containing only time-series samples and *less than specified discharge* ratings, removing any samples collected at discharges that could be considered events. Concentrations will be applied to their respective discharges. The use of the two methods in conjunction with each other in this study is for the purpose of validation of the fluxes calculated.

A quasi-continuous data set from 2003 to 2010 is available which contains data on hydrological and hydrochemistry conditions for both sites. In addition, a major restoration project occurred at the eroded sub-catchment, beginning in October 2007 and completed in May 2010. Previous work has utilised these parameters as a surrogate for peatland quality (e.g. Holden, et al., 2004; Jones, 2004; Holden, et al., 2007; Clark, et al., 2008; Shuttleworth, et al., 2019). Thus, use of these parameters can be used to try and subjectively infer the organic carbon flux in parallel with quantitative methods

As mentioned, organic carbon is a highly complex, heterogeneous mix of compounds usually considered source-specific (Nebbioso & Piccolo, 2013; Sillanpää, et al., 2014). Thus, there is a requirement to provide a degree of generilisation. Tangetial ultrafiltration (TFU) is a known method to separate carbon via physical size (Amon & Benner, 1996; Everett, et al., 1999; Jackson, et al., 2012). In this study, carbon will be separated in four size classifications; <1>0.2 µm, <0.2 µm>50 kDa, <50>10 kDa and <10>3 kDa. Although, with this categorisation there is a requirement for them to relate to functionalitiy in the environment . Size and surface area are known to be analogous with each other and surface area is a control of organic carbon lability (Amon & Benner, 1996; Maizel & Remucal, 2017). Thus, the lability of size fractions can be used to observe the individual potential of carbon dioxide production.

A majoirty of the literature have only classified organic carbon in one form (dissolved organic carbon) when investigating lability (Miller & Zepp, 1995; Moody, et al., 2013; Pickard, et al., 2017; Brown, et al., 2018). Few studies provide a more in-depth characterisation; in Amon & Benner (1996), it was observed that high molecular weight (HMW) (>1 kDa) organic carbon compounds were more readily utilised than lower weight fractions (<1 kDa) by micro-organisms. Similarly, HMW organic carbon compounds were more likely to be degraded via photochemical reactions than their lighter counterparts (Jones, et al., 2016). In addition, many of these studies use very different methods to quantify carbon lability. In Amon & Benner (1996) a biological oxygen demand (BOD) sensor was used as a surrogate of carbon dioxide production. While in Moody et al. (2013), lability was quantified via the loss of organic carbon over time. Intra-comparison of data is more difficult when a variety of methods are utilised by different researchers. In this study, as in Brown et al. (2018), a non-dispersive infrared (NDIR) sensor will be used to continuously measure the carbon dioxide production from samples, a method that could standardise lability studies.

Few studies have focused on the quantification of direct carbon dioxide fluxes in upland catchments (e.g. Hope, et al., 2001; Palmer, et al., 2001; Billett, et al., 2004; Dawson, et al., 2004; Hope, et al., 2004; Billett, et al., 2007; Billett & Moore, 2008; Dinsmore & Billett, 2008; Johnson, et al., 2008; Johnson, et al., 2010). Many of these studies have not been able to provide high-resolution measurements over a temporal scale due to methodological constraints. Headspace analysis is a common method to quantify aquatic carbon dioxide fluxes (e.g. Hope, et al., 2001; Palmer, et al., 2001; Billett, et al., 2004; Dawson, et al., 2004; Hope, et al., 2004; Billett, et al., 2007). This method relies on the spot sampling during visits to a study site which constrains carbon dioxide flux estimations. The sample measurements are set in the context of the spatial and temporal conditions at the distinct point in time in which it was collected, leading to an bias flux estimate. Recently, a number of studies have utilised non-dispersive infrared (NDIR) sensors in an attempt to reduce errors and provide more representative carbon dioxide measurements (Dinsmore & Billett, 2008; Dinsmore, et al.,

2009; Johnson, et al., 2008; Johnson, et al., 2010). In Dinsmore & Billett (2008), a total carbon dioxide load of 1.25 tons over a four-month period was observed of which 71% occurred during discharge events, which further highlights the importance of using high-temporal resolution methods. A review by Johnson et al. (2010) assessed the equipment's applications and compared it against the standard headspace analysis method applied in previous carbon dioxide flux studies. In a high proportion of scenarios, the two methods were not significantly different from each other. Although the main distinguishing factor was the ability of the sensor to record *in-situ* direct continuous measurements of carbon dioxide in the environment it was applied in.

Objectives of this paper are as follows:

(i) Predict the variability of organic carbon fluxes in a climate warming scenario subjectively and quantitively.

(ii) Predict the variability of sub-micron particle size distributions in a climate warming scenario through identification of the spatial-temporal significance of each size fraction.

(iii) Determine how the indirect carbon dioxide flux will be affected by the lability of organic carbon.

(iv) Analyse continuous *in-situ* carbon dioxide concentrations at the sub-catchments, suggesting the main driver of fluctuation and predict how they may change in a climate warming scenario.

2.0 Methods

2.1 Site description

Study site was the Crowden Great Brook (National Grid Reference of the catchment outflows 07042 99590). The catchment is part of the National Trust High Peak Estate located in Southern Pennines, Peak District. Catchment comprises of 70% blanket bog in a 7 km^2 area (Lliguin, 2017). The catchment can be split up into two distinct sub-catchments (Fig. 1). One sub-catchment has been subject to extensive erosion (Evans, et al., 2006). The second catchment is an intact area of peat, vegetated with common peat-forming plant species; Sphagnum moss (Gaffney, et al., 2008). As sites are located in close proximity to each other it is assumed similar metrological and hydrological conditions are experienced.

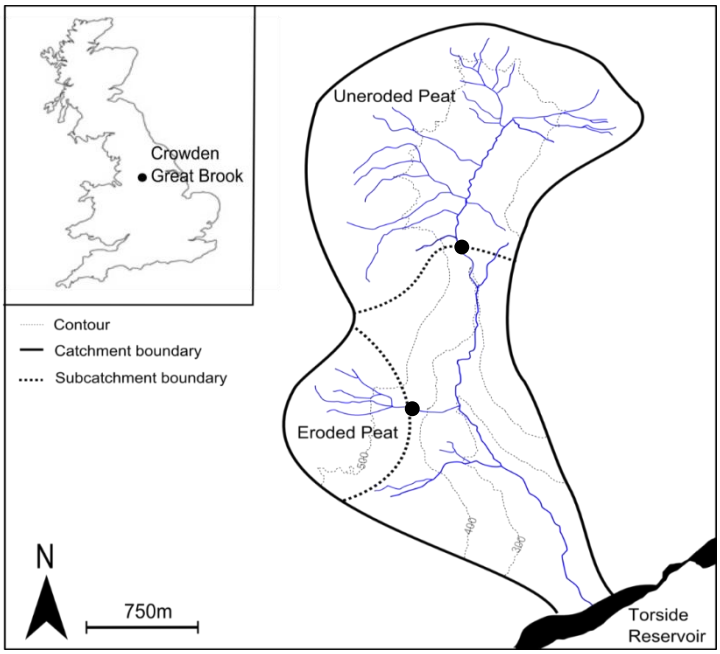

Figure 1: Crowden Great Brook catchment map. Two distinct sub-catchments outlined by dotted lines. Black dots represent sample site locations (Boult, 2017).

2.2 Field measurements

2.2.1 Water sampling regime

Water samples were collected in 500 ml plastic bottles using a Sigma 900 automatic water sampler installed at the two sampling sites. Auto-samplers were pre-programmed to either an *event* or a *daily* sampling regime depending on the information required. The samplers were connected to pressure transducers located in-stream, automatically switching on once the stage reached a certain height triggered by an event. Once triggered, collection at hourly intervals over a 24 hour period occured. Samples collected during the *daily* regime were collected periodically over 24 days. Site visits were made on a monthly basis, in which bottles were collected, batteries changed and auto-samplers reset. All samples were returned to the laboratory and processed within 72 hours of collection and monitoring occured from early January 2017 to July 2019.

2.2.2 Water quality sensors

In this study, Sentek PI11 pH electrodes and Dynament Platinum series (0-5% Vol. CO2) non-dispersive infrared (NDIR) sensors (output 0–2,499 mV) were installed *in-situ* at each sampling site. Sensors were installed at a depth below the baseline discharge conditions of respective streams. The pH electrodes were connected to Sentry II data logger. NDIR sensors were housed in a hard plastic coloumn for protection against debris. A polytetrafluoroethylene (PTFE) membrane covered the bottom inlet which allowed carbon dioxide diffusion across the membrane but prevented water from entering. NDIR sensor were connected to Onset HOBO four-channel logger with all components held in a Fibox case. All loggers (including barometers) were synced to measure at 15-minute intervals (NDIR sensors changed to five-minute intervals after the first month of measurements). Batteries could only be changed during site visits, when visits were prolonged batteries died leading to gaps in data collection.

2.2.3 Stage, discharge and meteorology

Three barometers were installed at the study site; two located *in-situ* at the vegetated and eroded catchment and one situated *ex-situ* further downstream. Manual stage measurements and dilution gauges were conducted during monthly visits. Meteorological data was gathered by a rain gauge installed at the eroded catchment near to the sampling location (Fig. 1).

2.3 Lab measurements

2.3.1 Total organic carbon

Water samples were split in to two sets; unfiltered and filtered. Whatman Nitrate membrane filter papers (0.2 µm pore size) used for filtered samples. Subsequent samples measured within 48 hours, approximately 15 ml of sample extracted to measure total organic carbon (TOC) using a total organic carbon analyser (Shimadzu TOC-V CPN). Samples catergorised in to >0.2 µm (unfiltered) & <0.2 µm (filtered). They were summed together to make comparisons with previous work (Jackson, 2010; Phai, 2012).

2.3.2 Tangential flow ultrafiltration

Organic carbon samples were separated in to varying size fractions with a sequence of paired 0.2 µm, 100 kDa, 10 kDa, and 3 kDa cut-off plates using a Viviaflow 50 cross flow cassette system connected to a peristaltic pump head. Total organic carbon of filtrate-retentate monitored via UV-VIS absorption in conjunction with a humic acid standard calibration curve throughout the tangential flow ultrafiltration process. Resultant total organic carbon concentrations were used to produce mass balance calculations to determine when retentate and filtrate became stable across a specific cut-off plate. Once stable, cut-off plates were removed and replaced with the next cut-off plates in descending order of size. Deionised water (DIW) was passed through the system before each sample to ensure tubes were cleared of previous remnants. Run time was dependent on the quantity and quality of samples usually between 12–24 hours.

2.3.3 Carbon lability

Organic carbon lability was measured using a Dynament Platinum series (0-5% Vol. CO2) NDIR sensor (output 0–2,499 mV) connected to an Onset HOBO four-channel logger (measurement interval 1 second). The experimental vassal was a custom made plastic coloumn (volume: 110 cm^3) and a NDIR sensor head glued onto a cap which screwed to the top of the plastic coloumn to create an air-tight seal, which prevented leakages and exterior atmospheric influences. 50 ml of a selected size fraction was extracted and deposited in to the coloumn. Prior to closing the system, the sample was allowed to fully oxidize with the atmosphere for 20 minutes. The sample was stirred using a IKA lab disc magnetic stirrer throughout the oxidation and experimental period. Experiments were conducted over a 12 hour period. Two of the size classfications, <10> 50 kDa and <1> 0.2 µm kDa, collected from the vegetated sub-catchment were completed using a different plastic vassal, which was believed to be leaking (Fig. 16 1B & 1D). Samples could not be re-run as they had been used for other experiments.

2.4 Data analysis

2.4.1 Historic data

All data had already been converted to required units from previous conversion factors and assumed to be correct and accurate. Analysis of the data identified major gaps in many of the years. As this study relies on year to year comparisons, a complete data set during similar time frames is required. The time period selection was based on the most consistent and longest period available in multiple years. The three-month period of May, June and July were selected in the years 2003, 2009 and 2018 at the eroded catchment and 2003, 2010 and 2018 at the vegetated catchment. It would have been preferable if the sub-catchments did not differ in years (2009 & 2010), however, it was unavoidable due to the data-set constraints. Specific events chosen for comparison were selected on the basis of similar meteorological conditions and the subsequent responses i.e. height and duration of a discharge peak. All event dates

were matching for the two sub-catchments. Run-off coefficients in this study were calculated by volume of discharge (m^3) divided by volume of rain (m^3).

2.4.2 Discharge

Curvilinear stage-discharge rating curves were constructed using stage measurement and dilution gauges for each sub-catchment (March 2016 to June 2019) (See supporting information – Fig. S1 and S2). Ratings were used to convert continuous stage (cm) values to discharge (L/s).

2.4.3 Organic carbon flux

Three methods of organic carbon flux calculation were used in this project.

Method 1 – Interpolation

A well-known load calculation was used; "Method 2", (Walling & Webb, 1985)

$$L = K \sum_{i=1}^{n} \left(\frac{CiQi}{n}\right) \quad \text{(i)}$$

Eq. (i) presents "method 2." L represents the total flux (load), C_i the concentration (mg/L) for each sample associated with Q_i, discharge, n the number of samples, and K is the conversion factor to scale units.

Method 2 – Rating Relationship

Log transformations of discharge and concentration were conducted by constructing rating relationships. The $y = mx + c$ equation derived from the rating relationships were applied to discharges measurements at 15-minute intervals, where x is discharge (L/s) and y is organic carbon concentration (mg/L). Subsequent concentrations were multiplied by discharge to calculate flux (mg/s). A conversion factor was applied to scale to a whole year and convert units. Where relationships expressed negative gradients and subsequent concentrations were negative, the value was assumed to be zero. Cut-off range for "baseflow" were decided by two

factors. First, flow duration curves were analysed and it was decided subjectively at what constituted baseflow. Secondly, how the selected discharge ranges interacted with calculations, for example, for the vegetated catchment all baseflows <120 L/s resulted in a majority of the concentrations to be calculated as negative. In the <5 L/s range at the eroded catchment in 2017, a higher proportion of discharges were in the “high-flow” category than “baseflow”. The <50 L/s range was applied instead, but only for the 2017 year at the eroded catchment.

Method 3 – Particle size distribution interpolation via flow duration

The particle size distribution flux was calculated using flow duration curves of respective sub-catchments. Ranges were decided subjectively and split into four categories for each catchment. Vegetated discharge ranges, 0-20, 20-100, 100-250 and >250 L/s. Eroded discharge ranges, 0-10, 10-20, 20-50 and >50 L/s. The particle size distribution concentrations were categorised using these ranges and averaged (mg/L). Discharge ranges were applied to respective flow duration curves, discharge within respective ranges were summed. The sum of discharges (L/s) was converted to volume (L) and multiplied by the average concentration of the particle size distrubutions (mg/L). A conversion factor was applied to scale to a year and convert units.

2.4.4 Carbon dioxide concentrations

The NDIR sensor’s raw data units, millivolts (mV) were converted to parts per million (ppm). NDIR sensor output: 0–2,499 mV with 2.3 mV for every 1 unit of ppm. Carbon dioxide concentrations were assumed to be uniform throughout the stream channel due to the relative turbulent nature of the stream at the two sites.

2.4.5 Carbon lability

Raw data units, millivolts (mV) converted to parts per million (ppm). NDIR sensor output: 0-2,499 mV with 2.3 mV for every 1 unit of ppm. Parts per million (ppm) was converted to percentage of carbon oxidised via calculations described below:

$$V_{CO2} = \left[\frac{(ppm - atm)}{K}\right] \times Hspace \quad \text{(ii)}$$

Eq. (ii) presents conversion from ppm to CO_2 (ml). V_{CO2} (ml) represents volume of carbron dixoxide (CO_2), *ppm* the NDIR sensor reading at a given second, *atm* (ppm) the atmospheric CO_2 concentration (~400 ppm), *K* the converstion factor and $Hspace$ (ml) the headspace available given specific volume of sample.

$$M_C = \left[\frac{V_{CO2}}{V_m}\right] \times m_a \quad \text{(iii)}$$

Eq. (iii) presents conversion from CO_2 (ml) to a mass of carbon (mg). M_C represents mass of carbon (mg) at a given second, V_{CO2} (ml) the volume of CO_2, V_m the molar volume of CO_2 at standard pressure and temperature and m_a is the atomic mass of carbon.

$$\%C = \left[\frac{M_C}{M_S}\right] \times 100 \quad \text{(iv)}$$

Eq. (iv) calculates the percentage of carbon oxidised over the experiment period. $\%C$ represents amount of carbon oxidised (%), M_C the mass of carbon (mg) at a given second and M_S is the mass of carbon in the sample (mg).

3.0 Results

3.1 Rating relationships

Cut-off ranges for baseflow used in rating relationships are highlighted in Fig. 2A and 2B. Rating relationships used to calculate fluxes are presented in Fig. 3 and 4. At the vegetated catchment, event rating relationships were positive for both size classes; >0.2 µm (r^2 = 0.42, $p < 0.05$) (Fig. 3A) and <0.2 µm (r^2 = 0.040, p = .30) (Fig. 3B). The <0.2 µm classification was not significant during an event. The baseflow rating for sizes, >0.2 µm and <0.2 µm, had negative relationships; (r^2 = 0.058, p = .18) (Fig. 3C) and (r^2 = 0.18, $p < 0.05$) (Fig. 3D), respectively with the >0.2 µm not significant during baseflow. At the eroded catchment, event rating linear relationships were positive for the two size classes; >0.2 µm (r^2 = 0.38, $p < 0.05$) (Fig. 4A) and <0.2 µm (r^2 = 0.44, $p < 0.05$) (Fig. 4B), with both size classifications being significant during an event. The <50 L/s baseflow rating; the >0.2 µm fraction had a negative linear relationship (r^2 = 0.0003, p = .87) (Fig. 4C). In contrast to the <0.2 µm rating which had a positive linter relationship (r^2 = 0.18, $p < 0.05$) (Fig. 4D) and the >0.2 µm classification was not significant at this discharge range. Similarly, the <5 L/s range, the >0.2 µm fraction had a negative linear relationship (r^2 = 0.006, p = .75) (Fig. 4E) and the <0.2 µm rating had a positive linear relationship (r^2 = 0.0561, p = .12) (Fig. 4F), neither were significant at this discharge range.

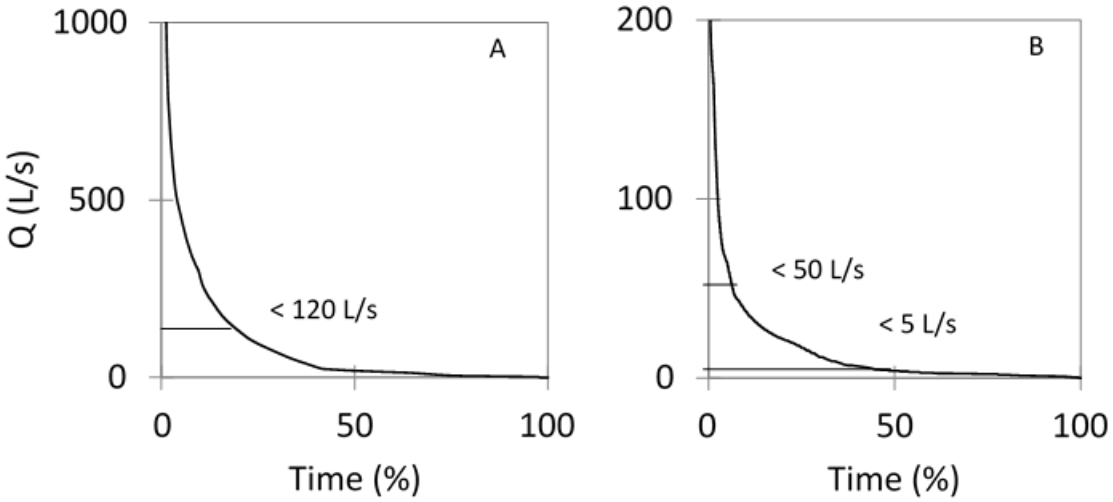

Figure 2: Flow duration curves of all discharge between 2003 to 2019 marked with cut-off ranges for baseflow used in rating relationships. A) Vegetated catchment B) Eroded catchment.

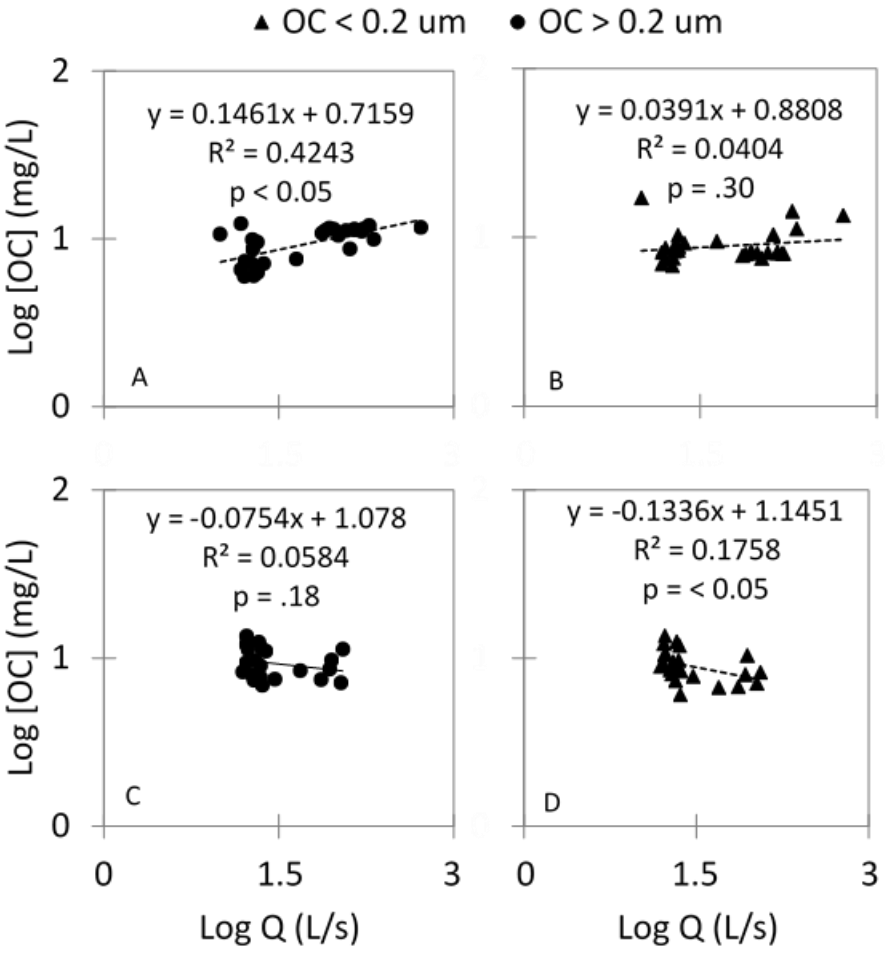

Figure 3: Vegetated catchment rating relationships of log OC (mg/L) concentration against log discharge (L/s). A) event time series >0.2 µm B) event time series <0.2 µm (n = 29) C) <120 L/s cut-off >0.2 µm D) <120 L/s cut-off <0.2 µm (n = 32).

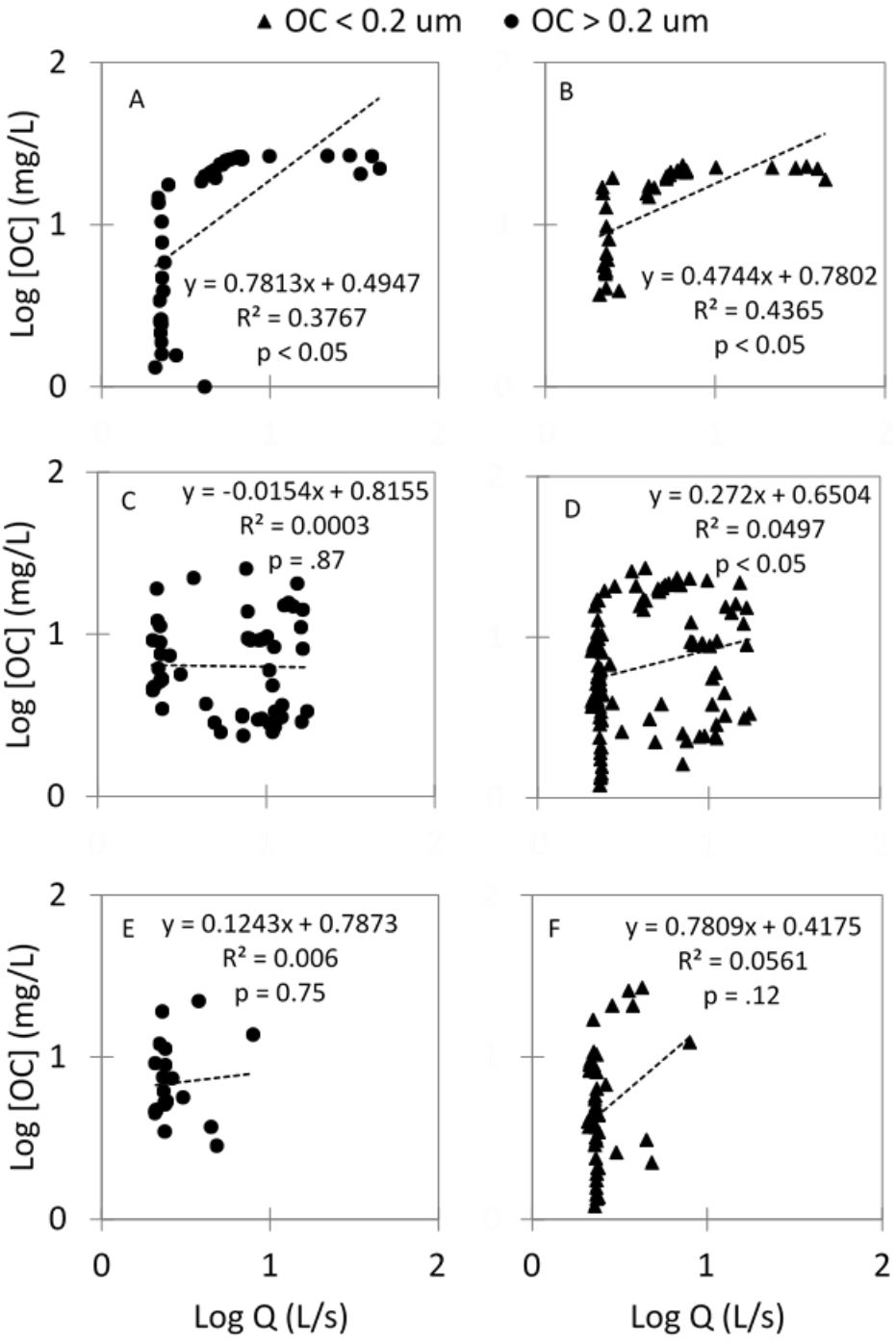

Figure 4: Eroded catchment rating relationship of log OC (mg/L) concentration against log discharge (L/s) A) event time series >0.2 µm (n = 40) B) <0.2 µm (n = 38) C) <50 L/s cut-off >0.2 µm (n = 86) D) <50 L/s <0.2 µm (n = 117) E) <5 L/s cut-off >0.2 µm (n = 20) F) <5 L/s cut-off <0.2 µm (n = 43).

3.2 Hydrological & water chemistry comparisons

3.2.1 Hydrological

3.2.1.1 Flow duration & rain duration curves

Rain duration and flow duration curves are presented in Fig. 5. In 2003, over May, June and July the total rainfall was 359 mm. Rainfall duration was not considerably different for the vegetated and the eroded catchment, 19.27% and 19.03%, respectively (Fig. 5 1C & 2C). Although, the percentage of time in which most of the water was moving differed between the two catchments. At the vegetated catchment, 93% of the water was moving in 25% of the time. In contrast, at the eroded catchment 85% of the water was moving in 12% of the time (Fig. 5 1A & 1B). In 2018, total rainfall was 82 mm, and comparably to 2003 rainfall durations were not considerably different between the catchments; vegetated catchment 3.7% and eroded catchment 4.0%, respectively (Fig. 5 1D & 2D). Flow duration was significantly lower in 2018 compared to 2003, likely due to the lower volume of rain. At the vegetated catchment, high flow accounted for 11% of the total discharge in 4% of the time (Fig. 5 2A). At the eroded catchment, discharge is observed to spend 99% of the time at what was considered baseflow in 2003 (Fig. 5 2B).

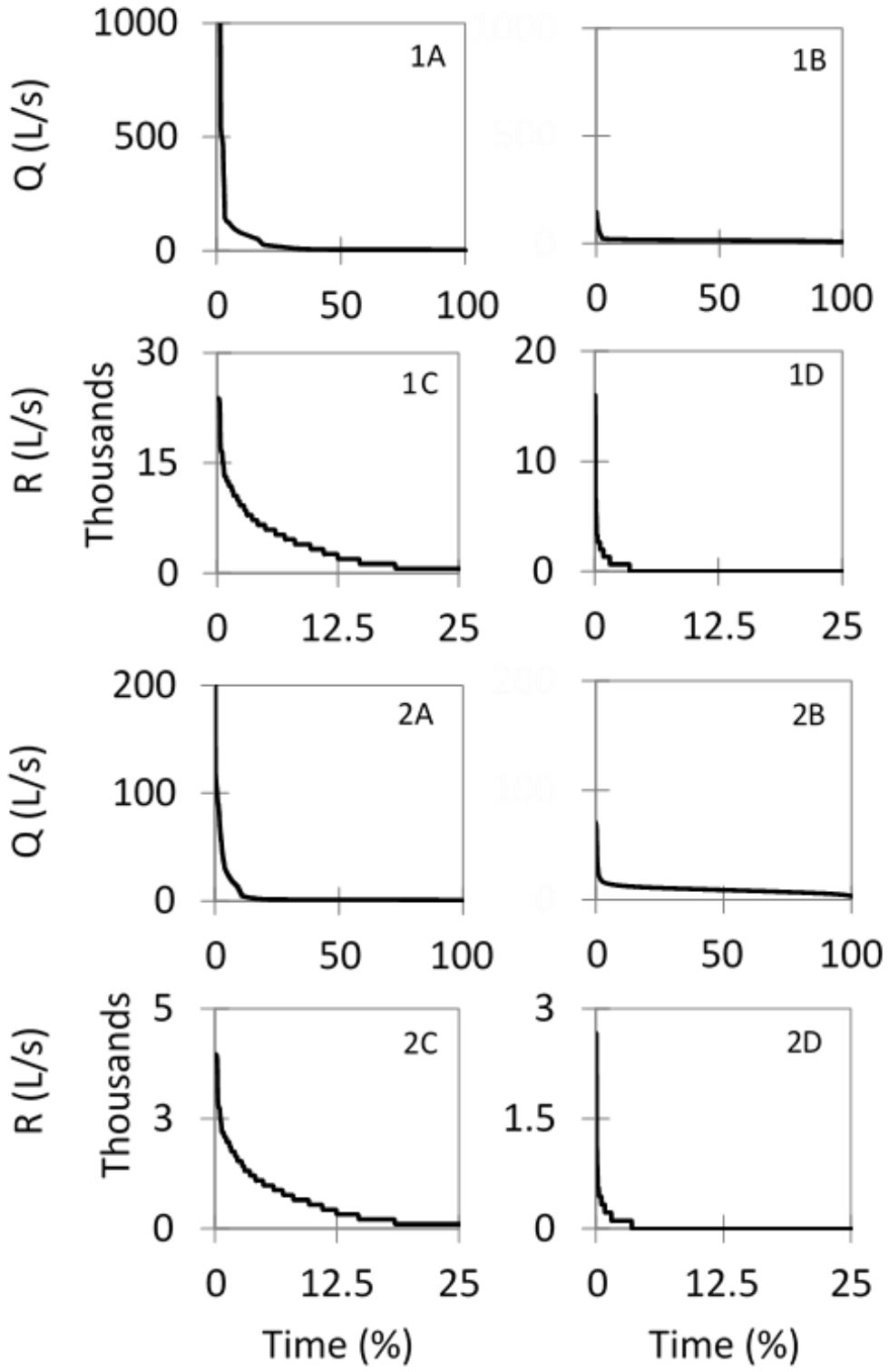

Figure 5: Vegetated and eroded catchments flow duration (FD) and rain duration (RD) curves in May, June and July in 2003 and 2018. 1A) Vegetated catchment FD (2003) 1B) Vegetated catchment FD (2018) 1C) Vegetated catchment RD (2003) 1D) Vegetated catchment RD (2018) 2A) Eroded catchment FD (2003) 2B) Eroded catchment FD (2018) 2C) Eroded catchment RD (2003) 2D) Eroded catchment RD (2018).

3.2.1.2 Run-off coefficient

Run-off coefficients for May, June and July are presented in Fig. 6. All run-off coefficients are <1. Run-off coefficients for the vegetated catchment remain uniform through the years from 0.25 in 2003 to 0.34 in 2009 and 0.30 in 2018. In comparison, run-off coefficients for the eroded catchment increase through proceeding years from 0.16 in 2003 to 0.33 in 2010 and 0.49 in 2018.

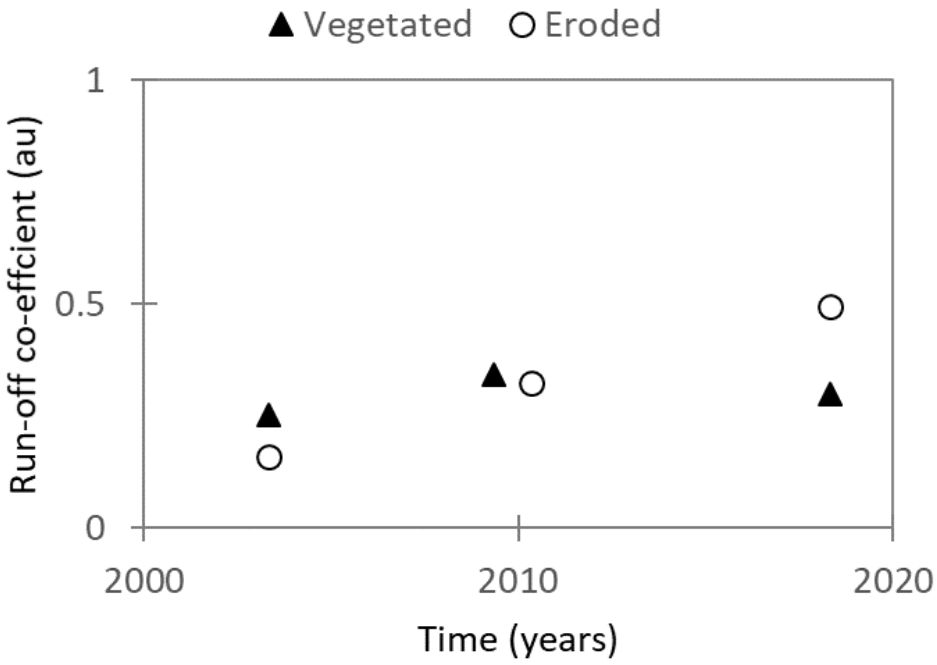

Figure 6: Run-off coefficients of months May, June and July for the vegetated and eroded catchment from 2003 to 2018 (n = 3).

3.2.1.3 Event run-off coefficient & discharge time to peak

Run-off coefficients and time to peak for events are presented in Fig. 7A & 7B. Mean run-off coefficient values are contrasting at the vegetated and eroded catchments; 0.38 and 0.20, respectively. In Fig. 7A, two events in 2003 and 2009 at the vegetated catchment (circled) likely contributed to the higher mean, 83% and 52% higher than their eroded counterparts. Aside from the two events, coefficients are relatively similar year to year. In 2019, there is a significant decrease in the eroded catchment run-off coefficient (0.014). In the time to peak plot (Fig. 7B), the two abnormal events at the vegetated catchment are not observed, unusual as a run-off coefficient would be associated with a high rate of water movement through the system. Time to peak at the eroded catchment was on average 1 hour faster than the time to peak at the vegetated catchment. In 2019, time to peak at both catchments exceeded 10 hours.

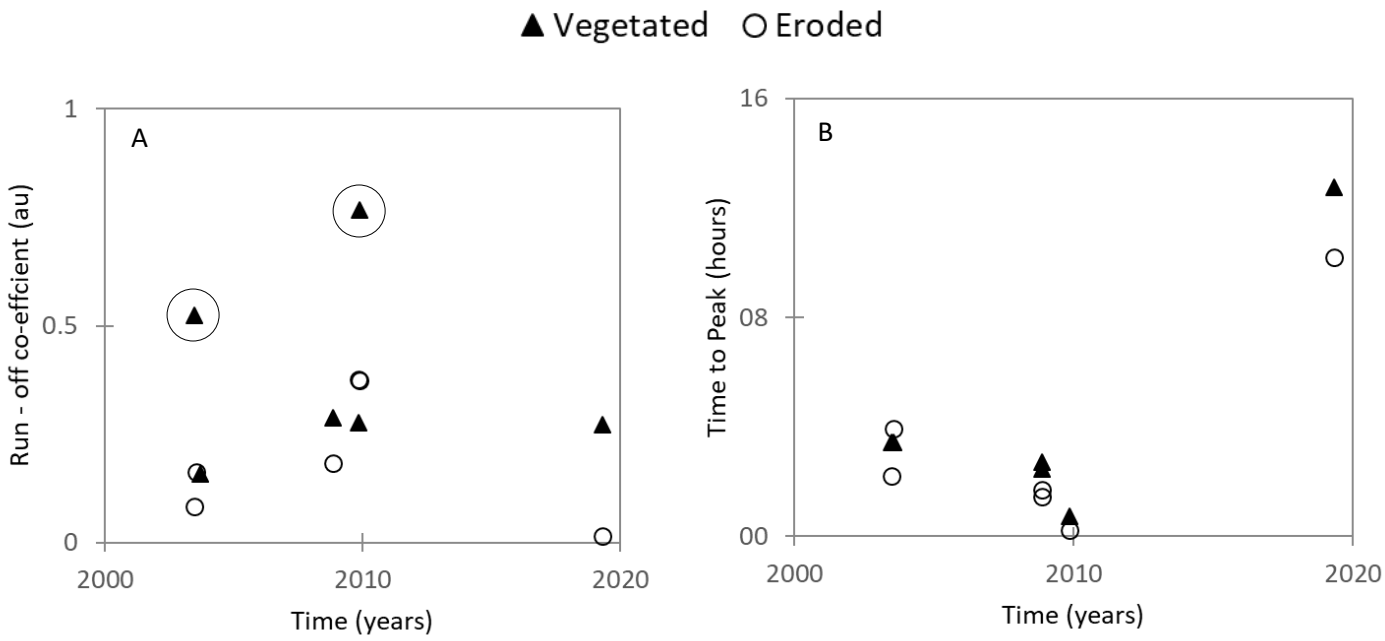

Figure 7: Run-off coefficients and time to peak for individual events at the vegetated and eroded catchmments (2003 to 2019) A) Run-off coefficients for individual discharge events B) Time to peak (hours) of individual discharge events (n = 8).

3.2.1.4 Cumulative discharge & rain event curves

Cumulative discharge and rain plots are present in Fig. 8. In 2003, the vegetated catchment discharge is observed to be more responsive to the increase in rain (Fig. 8 1A), while the eroded catchment, discharge does not appear to respond to rainfall (Fig. 8 2A). In 2008, in contrast to 2003, the vegetated catchment discharge response characteristics differ, discharge continues to increase with no decrease in gradient observed (Fig. 8 1B). At the eroded catchment, the response of discharge in 2008 correlates with rainfall more than in 2003 (Fig. 8 2B). The event in 2009 at the eroded catchment, appears to be the only event in which discharge is more responsive to rain than the vegetated catchment, with a much greater gradient in the discharge curve (Fig. 8 1C & 2C). The eroded catchment response to rainfall in 2019 was comparable to 2003 (Fig. 8 2A & 2D). Whilst the response at the vegetated catchment in 2019 was comparable to 2009 (Fig. 8 1C & 1D).

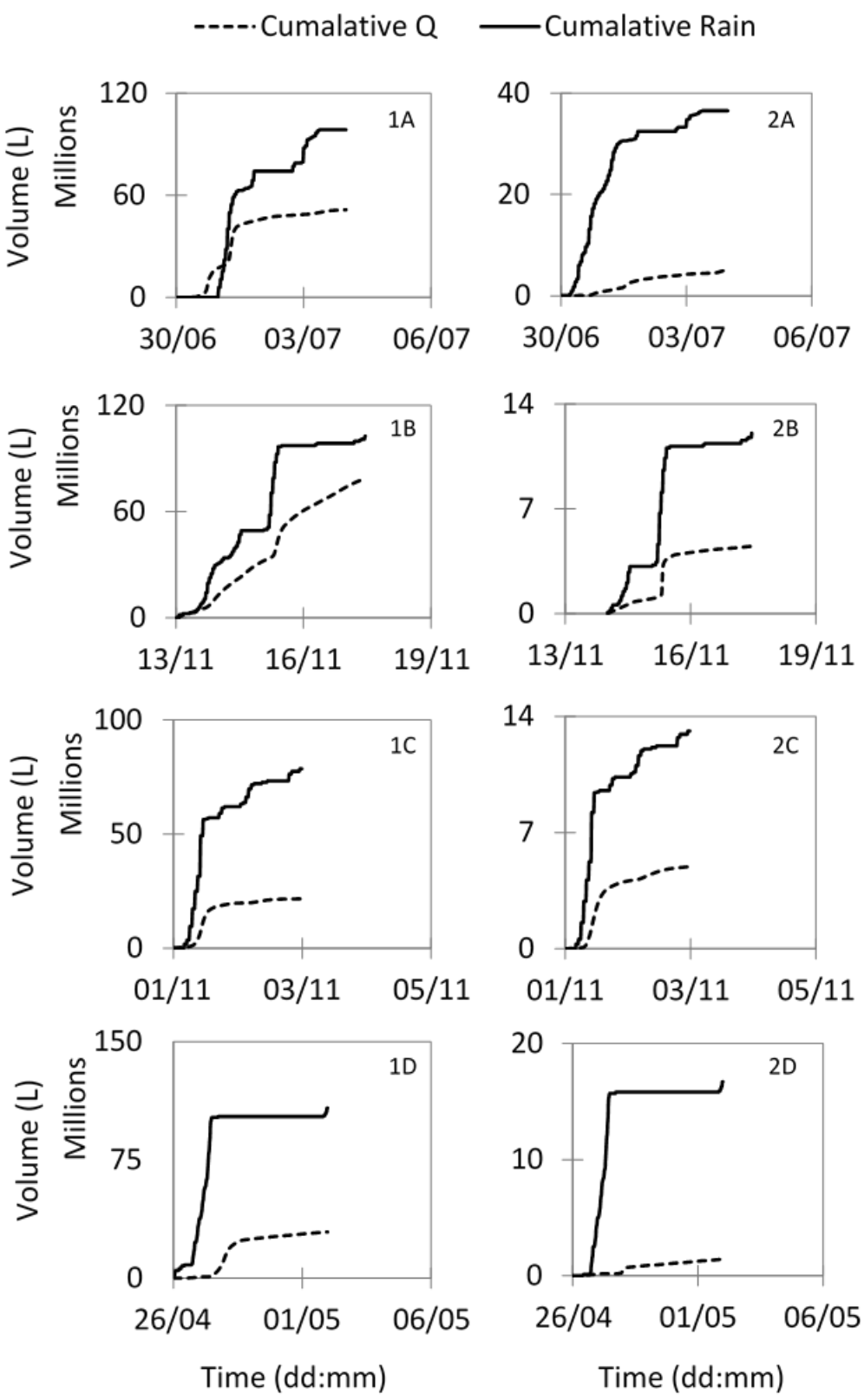

Figure 8: Cumulative rain (L) and discharge (L) plots for the vegetated and eroded catchments for individual events in 2003, 2008, 2009 and 2019. 1A) Vegetated catchment (2003) 1B) Vegetated catchment (2008) 1C) Vegetated catchment (2009) 1D) Vegetated catchment (2019) 2A) Eroded catchment (2003) 2B) Eroded catchment (2008) 2C) Eroded catchment (2009) 2D) Eroded catchment (2019).

3.2.2 Water chemistry

3.2.2.1 pH duration curves

Vegetated and eroded catchment pH duration curves for May, June and July are presented in Fig. 9. In 2003, pH ranged from 3.97 to 8.19 (mean 6.13) with a total discharge of 294,805 m^3 (data not shown) and from 4.28 to 7.08 (mean 6.07) with a total discharge of 36,609 m^3 (data not shown) for the vegetated and eroded catchment, respectively (Fig 9 1A and 2A). The pH in both catchments was >5 for 80% of the time. In comparison, pH in 2019 ranged from 3.75 to 6.68 (mean 5.97) with a total discharge of 339,658 m^3 (data not shown) and 3.54 to 6.69 (mean 5.96) with a total discharge of 34,771 m^3 (data not shown) at the vegetated and eroded catchment, respectively. The pH was sustained at >5 for 90% of the time at both catchments, compared to 80% in 2003.

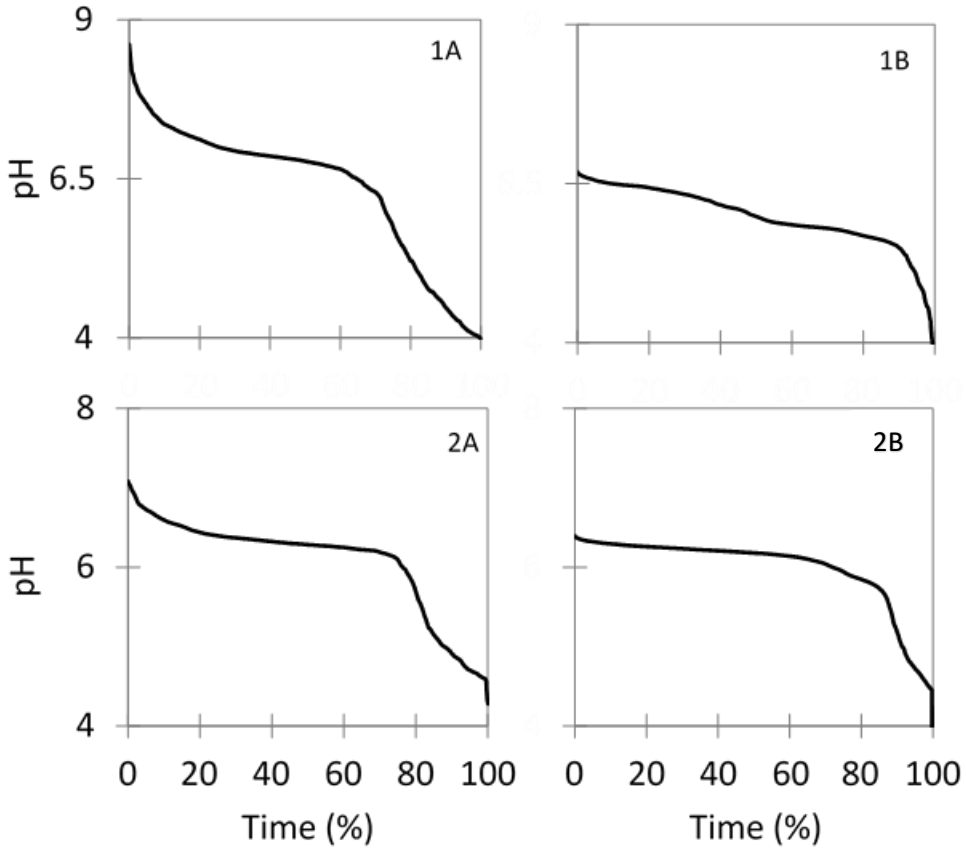

Figure 9: Vegetated and eroded catchments pH duration curves for the months of May, June and July in 2003 and 2019. 1A) Vegetated catchment pH duration curve (2003) 1B) Vegetated catchment pH duration curve (2019) 2A) Eroded catchment pH duration curve (2003) 2B) Eroded catchment pH duration curve (2019)

3.2.2.2 Event pH time to peak

Vegetated and eroded catchment pH time to peak are presented in Fig. 10. Analysis indicated that average time to peak was not considerably different between the two catchments, with 2 hours for the vegetated and 1 hour 45 minutes for the eroded catchment. However, from 2003 to 2019 time to peak remains similar at the eroded catchment while the time to peat at the vegetated catchment dropped to 1 hour shorter.

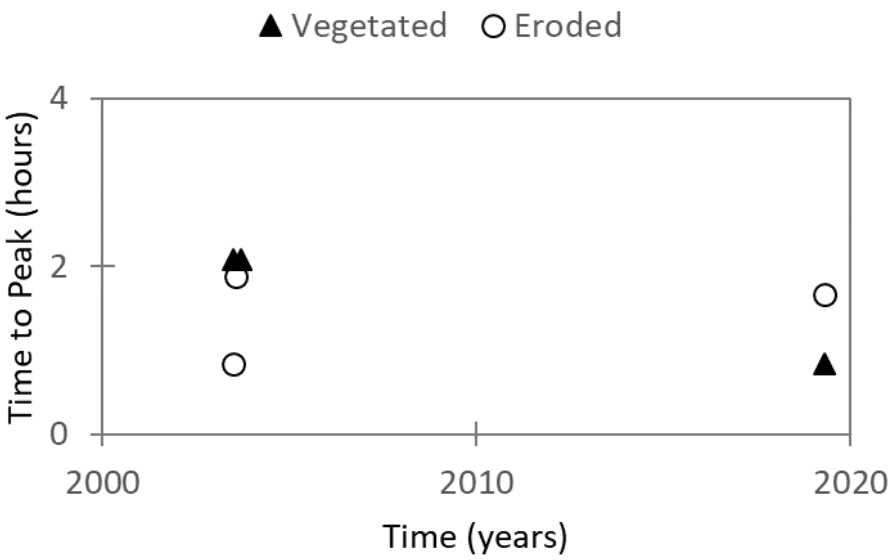

Figure 10: Vegetated and eroded events pH time to peak of pH against years in 2003 to 2019 (n = 3)

3.2.2.3 Cumulative pH & rain event curves

Stream H^+ concentration, rain H^+ concentration and discharge volume cumulative curves are presented in Fig. 11. In 2003, stream H^+ increased prior to discharge at the vegetated catchment, in comparison stream H^+ concentrations at the eroded catchment were much more responsive to discharge (Fig. 11 1A and 2A). The response of the vegetated catchment would indicate an influence of pH from rainfall, observed in Fig. 11 1B, the stream H^+ (mol) increase after the rainfall H^+ (mol). Although rain H^+ input and the stream H^+ magnitudes are very contrasting; 1.6 million mol to 300 mol, respectively. This is comparable to the eroded catchment in which the stream H^+ and the rainfall H^+ input are 5,000 mol and 60 mol, respectively (Fig. 11 2B). In 2019, compared to 2003 stream H^+ concentrations have a greater response to discharge at the vegetated catchment, while stream H^+ concentrations in the eroded catchment start highly responsive to discharge but diverge with time, continuing with an unusual gradient (Fig. 11 1C and 2C). In both catchments, the difference between the stream H^+ (mol) and rain H^+ input are comparable to 2003 (Fig. 11 1D and 2D). The difference in magnitudes observed suggest that the rain H^+ (mol) input will only have a minor influence on the stream H^+ (mol) and a majority is from terrestrial sources.

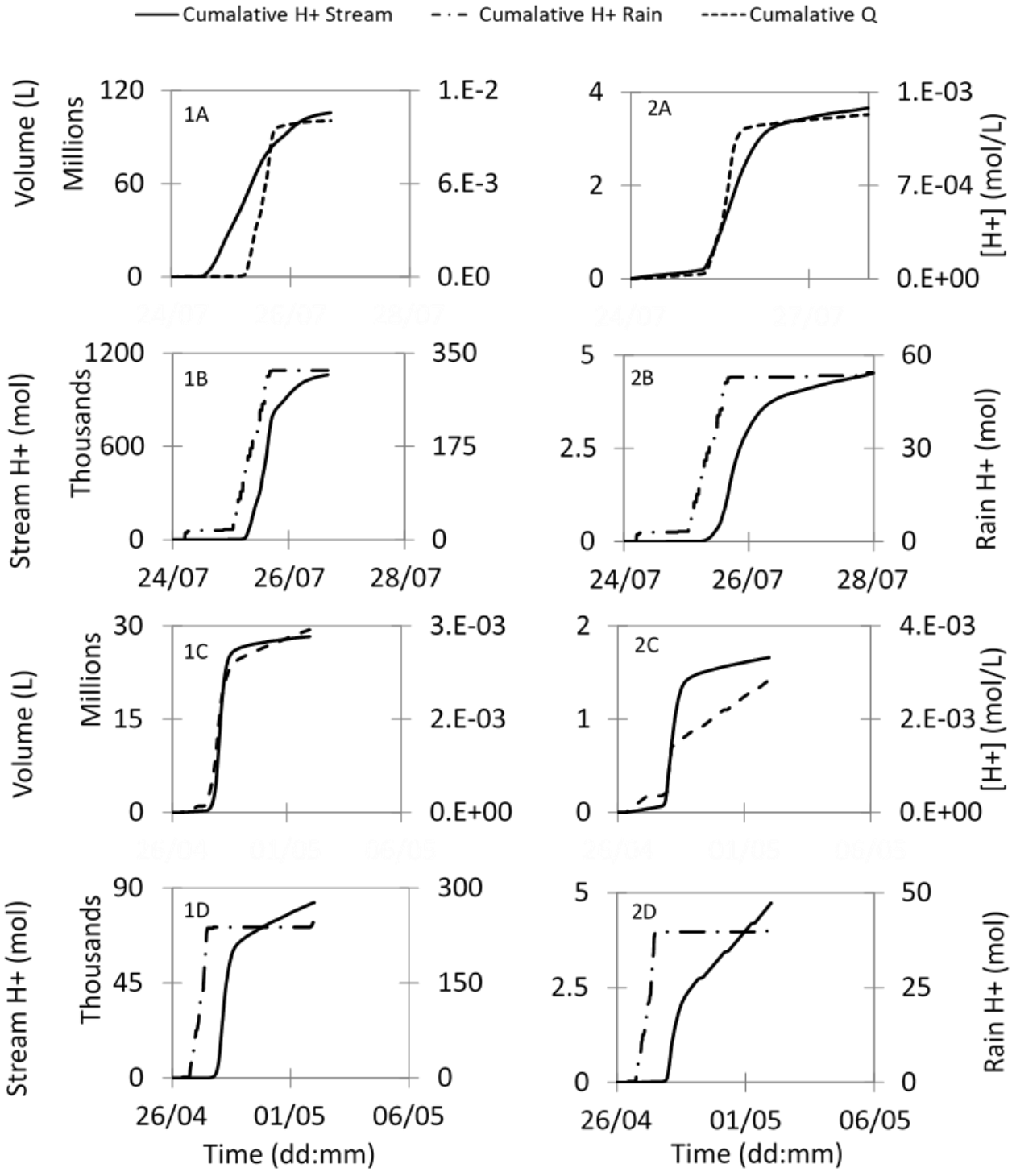

Figure 11: Cumulative stream H^+, discharge and rain H^+ plots of two events in 2003 and 2019. Numerical labelling represents 1) Vegetated catchment 2) Eroded catchment. Alphabetic labelling represents A) Catchments cumulative stream H^+ (mol/L) and cumulative discharge (L) (2003) B) Catchments cumulative stream H^+ (mol) and rain H^+ (mol) (2003) C) Catchments cumulative stream H^+ (mol/L) and cumulative discharge (L) (2019) D) Catchments cumulative stream H^+ (mol) and rain H^+ (mol) (2019).

3.2 Organic carbon flux

3.2.1 Previous work & current study

Organic carbon concentrations used to calculate fluxes plotted in an unrepresented year are presented in Fig. 12 A and B (event organic carbon concentrations not included), which is a visual aid to readers to show how representative the study data was over a year. The vegetated catchment had the lowest spread over seasons, with concentrations from summer and winter absent (Fig. 12A). In comparison, for the eroded catchment organic carbon concentrations from only winter were absent. Furthermore, an increase in organic carbon concentrations can be observed beginning in summer (Fig. 12B), while they remain constant at the vegetated catchment. Table 1 provides further details on the data that was used for the two methods of calculation in Jackson (2010), Phai (2012) and the current study.

Organic carbon fluxes calculated by interpolation were considerably lower in previous work by Jackson (2010) and Phai (2012) compared to the current study (Fig. 13A). An exception is 2008, where the vegetated catchment organic carbon flux is substantially higher than in all previous and current monitoring years. In both Jackson (2010) and Phai (2012), the eroded carbon flux is unexpectedly lower than the vegetated between 2006 to 2009. An exception is 2010, where the flux is greater but only by 0.21 t km^{-2} $year^{-1}$. Only between 2017 to 2019 the eroded catchment fluxes become considerably greater than the vegetated catchment fluxes, which is consistent for all three years. In comparison to the previous studies in which the vegetated catchment was mostly greater than the eroded catchment. Throughout 2017 to 2019 the average interpolation flux for the eroded catchment was 36.1 t km^{-2} $year^{-1}$. In contrast to 2006 to 2009 in Jackson (2010) and 2008 to 2010 in Phai (2012) (4.9 t km^{-2} $year^{-1}$ & 6.97 t km^{-2} $year^{-1}$, respectively), which are considerably lower. Similarly the rating relationship calculations by Jackson (2010) were lower than the flux observed in the current study (Fig. 13B). The flux increases from 5.26 t km^{-2} $year^{-1}$ (2006 to 2009) to 21.83 t km^{-2} $year^{-1}$ (2017 to 2019). There is discrepancies between the two methods of calculation in the current study, total interpolated fluxes at the vegetated and eroded catchments were 17.57 t km^{-2} $year^{-1}$ and

108.30 t km^{-2} $year^{-1}$, respectively. In contrast to the rating relationship estimates which were 31.75 t km^{-2} $year^{-1}$ and 65.48 t km^{-2} $year^{-1}$, respectively (Fig. 13 A and B).

Table 1: Information used to calculate fluxes from previous studies and current study (2003 to 2019). "*" refers to absent information.

	VEGETATED		ERODED		DATA OBTAINED FROM
YEAR	Days of data	Data points	Days of data	Data points	
2006	210	4	241	4	(Jackson, 2010)
2008	212	8	104	8	(Jackson, 2010)
2008	*	7	*	4	(Phai, 2012)
2009	339	19	339	19	(Jackson, 2010)
2009	*	18	*	20	(Phai, 2012)
2010	*	149	*	172	(Phai, 2012)
2017	239	17	239	37	
2018	364	44	364	50	
2019	154	71	154	72	

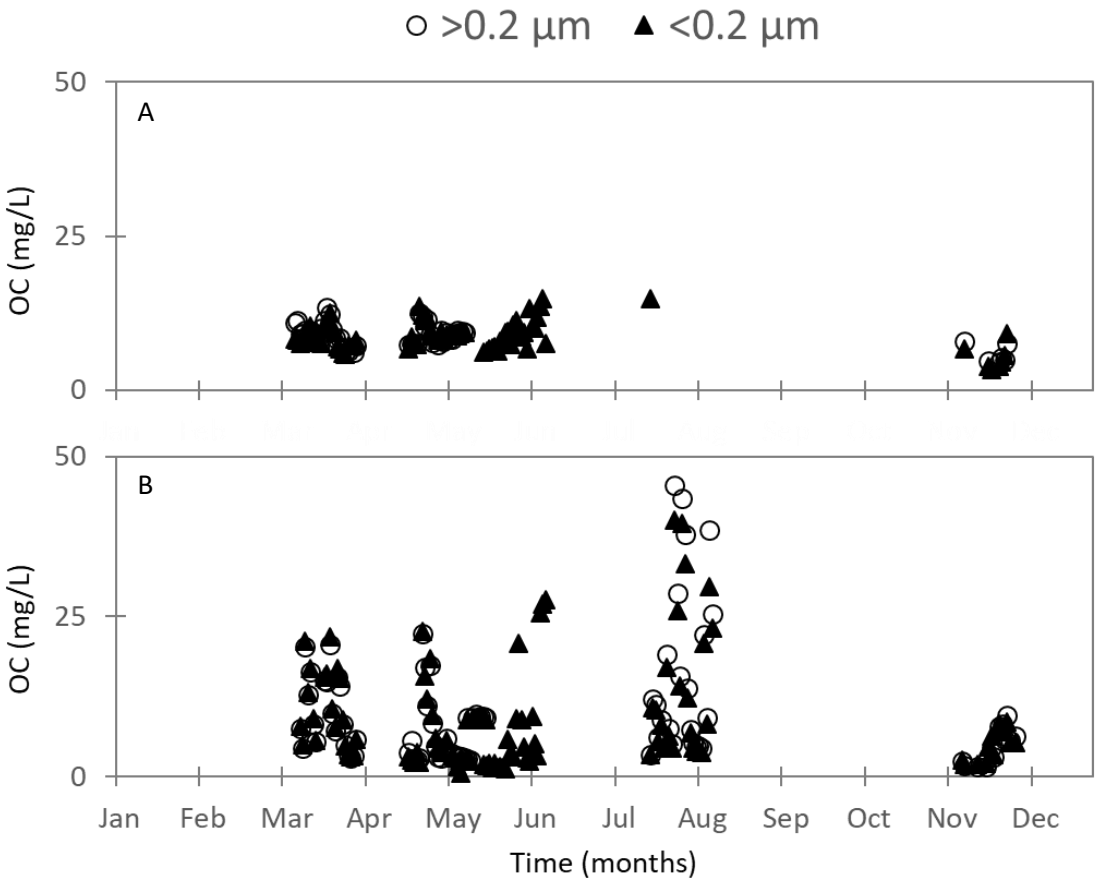

Figure 12: Vegetated and eroded time series of sample OC concentrations (mg/L) collected between 2017 to 2019 regardless of year collected. A) Vegetated catchment (n = 76) B) Eroded catchment (n = 111). Event samples not included as high temporal resolution would have made observation more difficult.

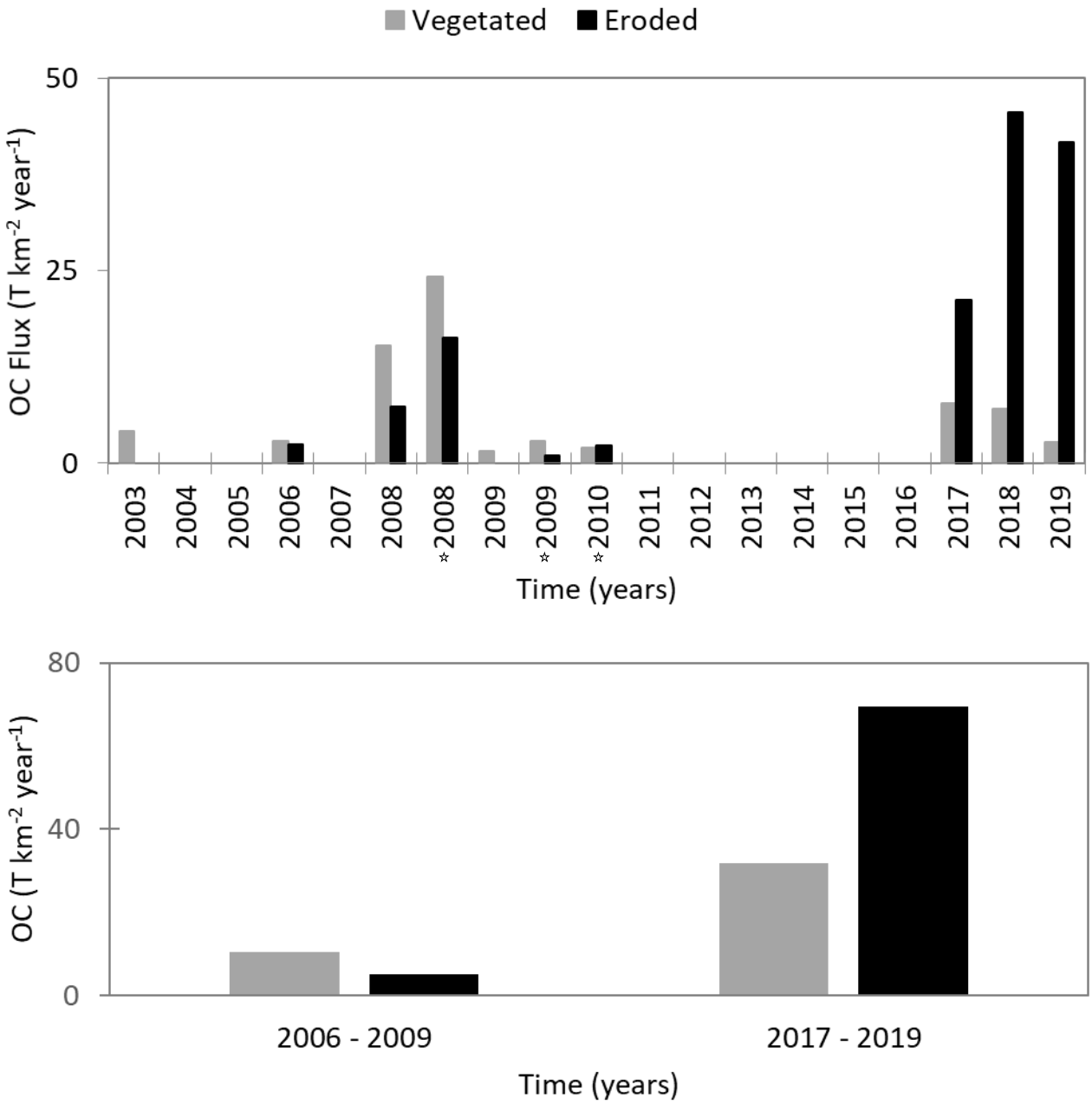

Figure 13: Vegetated and eroded catchments organic carbon flux time series calculated via interpolation and rating relationship methods from 2003 to 2019 A) Organic carbon flux time series calculated via interpolation calculations (2003–2019) ("*" distinguishes Phai (2012) study from Jackson (2010)) B) Organic carbon flux calculated via rating relationships compared to Jackson (2010) (Jackson (2010) study summed 2006 to 2009 fluxes together, this was also completed for 2017-2019 for comparability).

3.2.2 Sources of error

3.2.2.1 Direct comparison of interpolation and rating calculations

Comparisons of the two methods are highlighted in Table. 2. The flux calculated via interpolation were consistently higher in relation to the rating method at both catchments. At the vegetated catchment the flux obtained by interpolation was approximately 200 times larger than the flux extrapolated via the rating relationship method. The difference between the two methods observed at the eroded catchment was not as extreme, with the interpolation flux being two times larger than the flux extrapolated via the rating method.

Table 2: Comparison of interpolation and rating relationship calculations using organic carbon concentrations (mg/L) collected during a 24-day sampling regime. Notice change of units of carbon flux from t km^{-2} $year^{-1}$ to kg day^{-1}

SITE	VEGETATED	ERODED
	OC flux (kg day^{-1})	OC flux (kg day^{-1})
INTERPOLATION	266.49	49.37
RATING RELATIONSHIP	1.53	22.01

3.2.2.2 Organic carbon hysteresis

Vegetated and eroded log time series and log rating relationships of an individual discharge event are presented in Fig. 14, highlighting the complex relationship that can arise between discharge and organic carbon concentrations throughout an event. In both events there is clear evidence of a rising and falling limb in carbon concentrations coinciding with the rise and fall of discharge (Fig. 14 1A & 2A). In the vegetated catchment a clockwise hysteresis pattern occurs (Fig. 14 1B), dilution of organic carbon concentrations by rain occurs before the velocity of surface run-off is high enough to mobilise peat material and flush it in to the system. Concentrations of both size fraction peaks do coincide with peak discharge and begin to decrease afterwards. In contrast, the eroded catchment presents an anti-clockwise hysteresis (Fig. 14 2B), material is mobilised with a lower velocity of surface run-off than the vegetated catchment, and thus organic carbon concentrations increase very rapidly in the stream. The two sizes both coincide with peak discharge and decrease with the lower velocity of discharge, likely the end of the rainfall event.

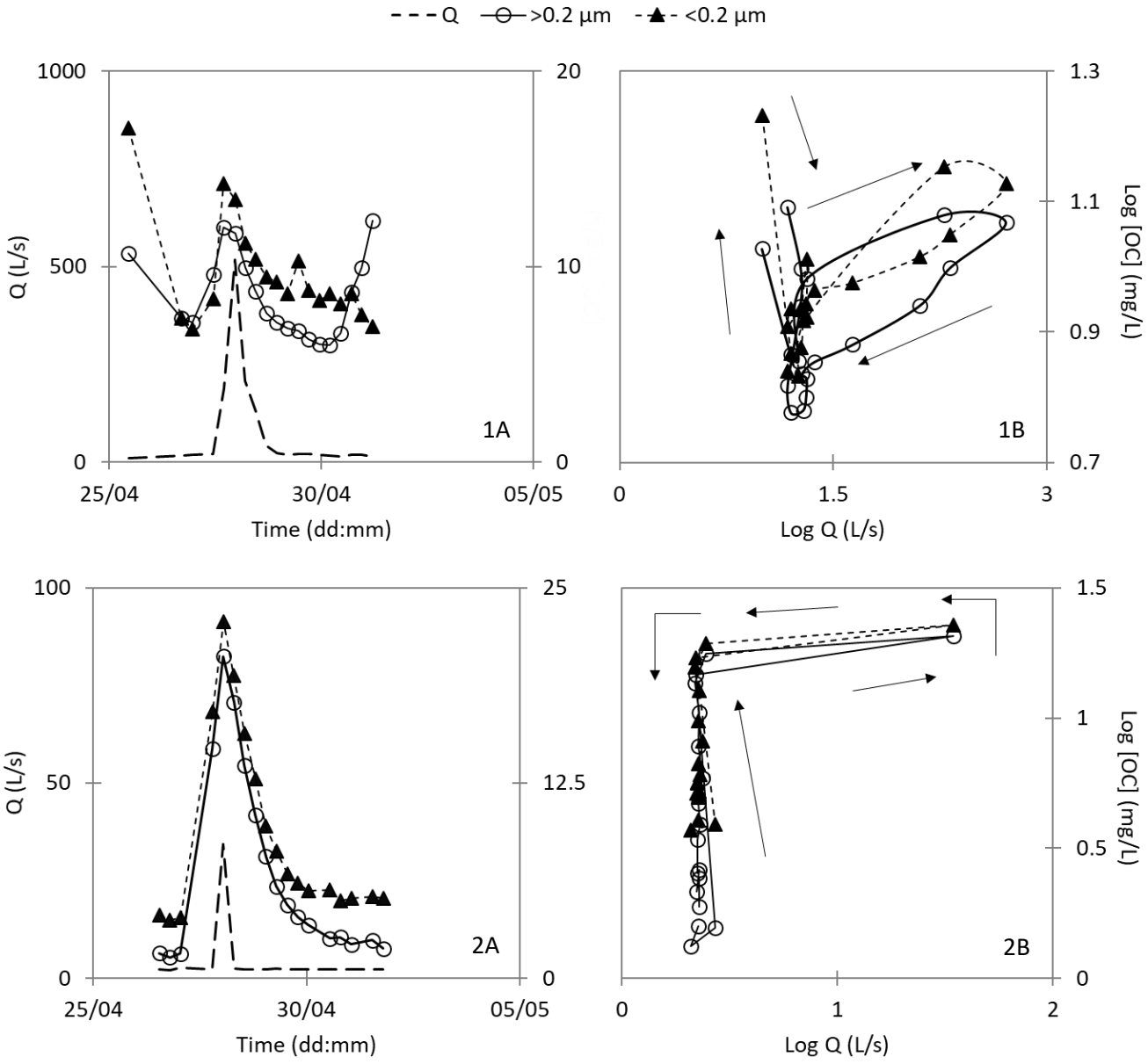

Figure 14: Vegetated and eroded catchments log time series and rating relationships of an individual event on 30/04/2019. 1A) Vegetated catchment log time series 1B) Vegetated catchment rating relationship 2A) Eroded catchment log time series 2B) Eroded catchment rating relationship. Note the axis on the rating relationships have been magnified.

3.3 Particle size distribution

3.3.1 Quantity

Particle size distributions of the two sub-catchments are presented in Fig. 15 1A and 2A. Material is observed to be larger when at the lowest discharge range at both catchments. An increase in discharge then causes the largest material to become less dominant. The smallest fraction (<3 kDa) constituting 54% and 43% of the particle size distribution at ranges 20–100 L/s at the vegetated catchment (Fig. 15 1A) and 10–20 L/s at the eroded catchment (Fig. 15 2A), respectively. A further increase in discharge causes the contribution of larger material to increase again. The smallest fraction (<3 kDa) contribution decreases to 17% and 10% at ranges >250 L/s at the vegetated catchment (Fig. 15 1A) and >50 L/s at the eroded catchment (Fig. 15 2A), respectively.

Discharge influence on the <10>3 kDa fraction differs at the two catchments. An increase is observed for the vegetated catchment, from 24% to 41% of the particle size distribution (Fig. 15 1A). In comparison, for the eroded catchment a decrease from 37% to 11% is observed (Fig. 15 2A). The two catchments particle size distributions contrasted at the highest discharge ranges. In the vegetated catchment at the >250 L/s range particle size distribution remained dominated by the <3 kDa & <10>3 kDa fractions (collective percentage: 58%), although, the proportion of larger material does increase (Fig. 15 1A). In contrast, the eroded catchment at the >50 L/s range is collectively dominated by the mid to large-size fractions <100>10 kDa & <0.2 µm>50 kDa constituting 23% and 37%, respectively. The two smallest fractions <3 kDa & <10>3 kDa are reduced to 20% collectively of the particle size distribution (Fig. 15 2A).

Flow duration curves highlight the spatial-temporal variability of water volume at the chosen ranges (Fig. 15 1B and 2B). Particle size distributions at the maximum discharge ranges occur only 11% and 9% of the time at the vegetated and eroded catchment, respectively. Although they constitute a small percentage of time the highest discharge ranges make-up 67% and 45% of the vegetated and eroded catchments total volume of discharge.

Size fraction fluxes are presented in Fig. 15C, the vegetated catchment had a greater flux than the eroded; 48.64 t km^{-2} yr^{-1} to 34.92 t km^{-2} yr^{-1}, respectively. In both catchments a positive relationship between discharge (m^3) and flux (t km^{-2} yr^{-1}) is observed. Although in the eroded catchment at the >50 L/s range a considerable decrease is observed from 23.43 t km^{-2} yr^{-1} to 4.70 t km^{-2} yr^{-1} (Fig. 15 2C). The quantity of the decrease is unexpected, as the amount of material is expected to always be larger than the vegetated catchment from previous analysis in Fig. 13, thus, the >50 L/s range will not be considered for comparisons, instead the 20-50 L/s range is used for the eroded catchment. The maximum discharge range for the total flux in the vegetated catchment (26.27 t km^{-2} yr^{-1}) is far greater than the eroded catchment (23.43 t km^{-2} yr^{-1}). In both catchments the flux proportions are comparable to the particle size distributions. The vegetated catchment flux is collectively dominated by the two smallest size fractions <10>3 kDa and <3 kDa, constituting 10.86 t km^{-2} yr^{-1} and 4.47 t km^{-2} yr^{-1}, respectively. Similarly, for the eroded catchment <10>3 kDa and <3 kDa fractions are dominant constituting 7.73 t km^{-2} yr^{-1} and 8.96 t km^{-2} yr^{-1}, respectively. The next largest flux is 4.46 t km^{-2} yr^{-1} from the <0.2 µm> 50 kDa fraction. Refer to Table 3 for further details on the volume of water and flow percentage time for chosen discharge ranges.

Table 3: Total volume of water (L) & time (%) of which it occurs for each discharge range of the vegetated and eroded catchment.

Vegetated catchment				
Discharge range (L/s)	0-20	20-100	100-250	>250
Volume (L)	6.E+08	4.E+09	5.E+09	1.E+10
Time (%)	51	25	13	11
Eroded catchment				
Discharge range (L/s)	0-10	10.-20	20-50	>50
Volume (L)	3.E+08	2.E+08	7.E+08	1.E+09
Time (%)	68	10	16	6

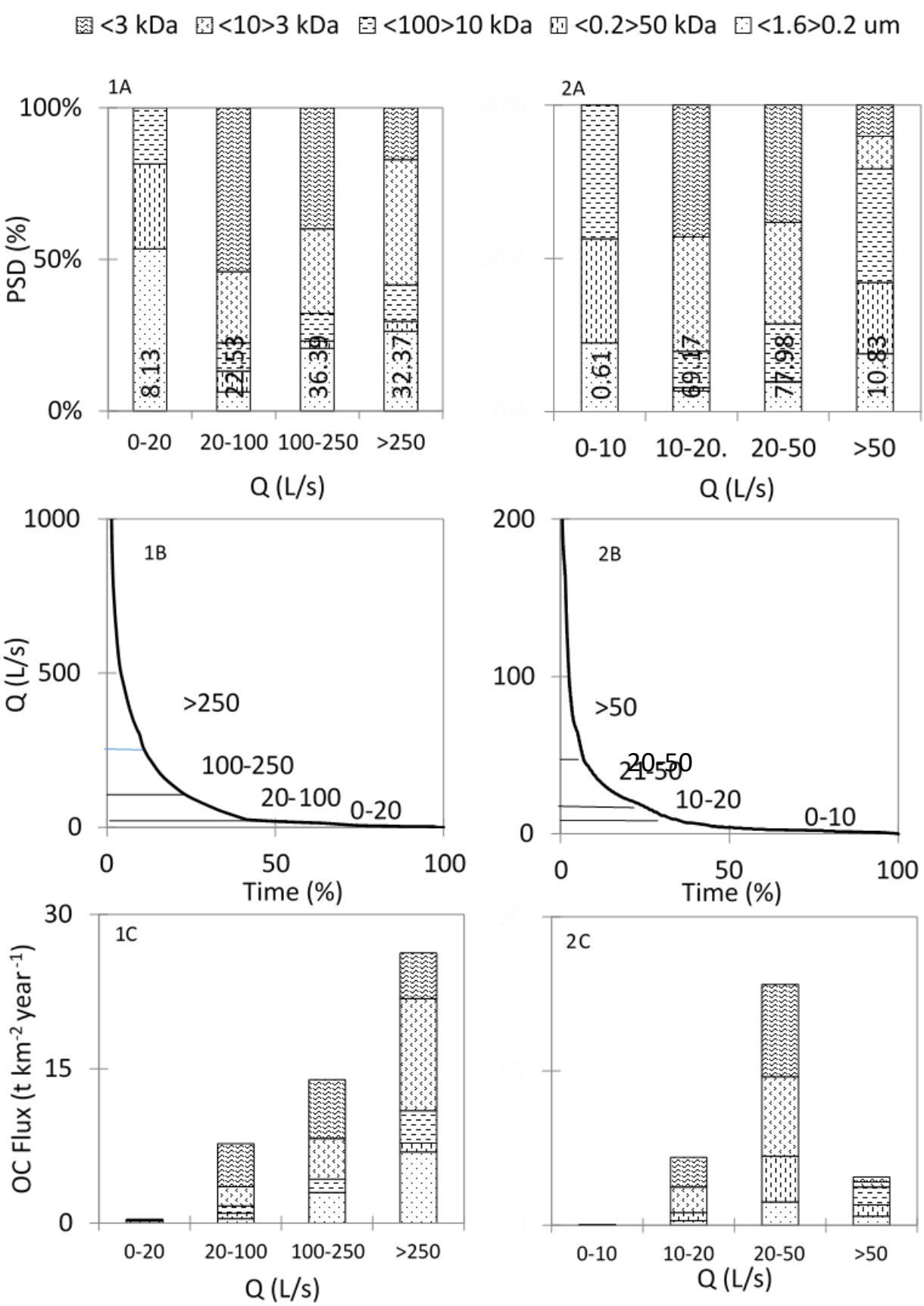

Figure 15: Particle size distributions for the vegetated and eroded catchments A) Average percentage particle size distribution categorised via discharge range (horizontal number within base of columns are the averaged organic carbon concentrations (mg/L)) B) Flow duration curves with discharge ranges highlighted with black line C) Fluxes of size fractions categorised via discharge range. Numerical labelling represents: 1) Vegetated catchment 2) Eroded catchment.

3.3.2 Quality

The two size classifications completed using a different experimental vassal were noticeably affected (Fig. 16 1B and 1D). In comparison to their corresponding size classification at the eroded catchment completed using the new vassal, the organic carbon oxidation curves were flattened, especially evident in the <0.2 µm>50 kDa fraction. For this reason, they will not be included in comparisons.

In oxidation experiments, the <1>0.2 µm fractions are considered controls. All fractions below this size should be sterile because bacteria will be destroyed during the tangential flow ultrafiltration separation process. When the sensor reaches the maximum output (curve flattens), the oxidative process is considered to be on-going but it cannot be considered. The variability of organic carbon concentrations had an effect on the percentage of oxidation and thus the calculated rate of oxidation. This is evident in both the vegetated and eroded catchments <0.2 µm>50 kDa fraction, which have the lowest organic carbon concentrations but the highest end-point oxidation percentages, 24% and 100%, respectively (Fig. 16 1C and 2C). Another analysis must be considered due to this, time taken to achieve senor maximum will be used as a surrogate of percentage oxidation. The shortest time to reach the sensor maximum will be assumed to have higher oxidation rates. From this evaluation method, a negative relationship between size and oxidation rate is observed. In both catchments the smallest fraction (<10>3 kDa) reached the maximum in <2 hours (Fig. 16 1A and 2A). For the vegetated catchment the total percentage carbon oxidised and the oxidation rate were 1.7% and 0.9% hr^{-1}, respectively (Fig. 16 1A). The eroded catchment had lower values for both total percentage carbon oxidised and oxidation rate, 0.7% and 0.3% hr^{-1}, respectively (Fig 16 2A). The <0.2 µm>50 kDa fraction from the vegetated catchment was the only other fraction that reached the maximum output in <7 hours, 24% of organic carbon was oxidised in 5 hours with an oxidation rate of 4.8% hr^{-1} (Fig 16 1C). All remaining size fractions reached maximum sensor output in >7 hours e.g. the <50>10 kDa total oxidation 1% and rate of 0.13% hr^{-1} (Fig.

16 2B) and <1>0.2 µm total oxidation 2.2% & oxidation rate of 0.23% hr^{-1} (Fig. 16 2D) at the eroded catchments .

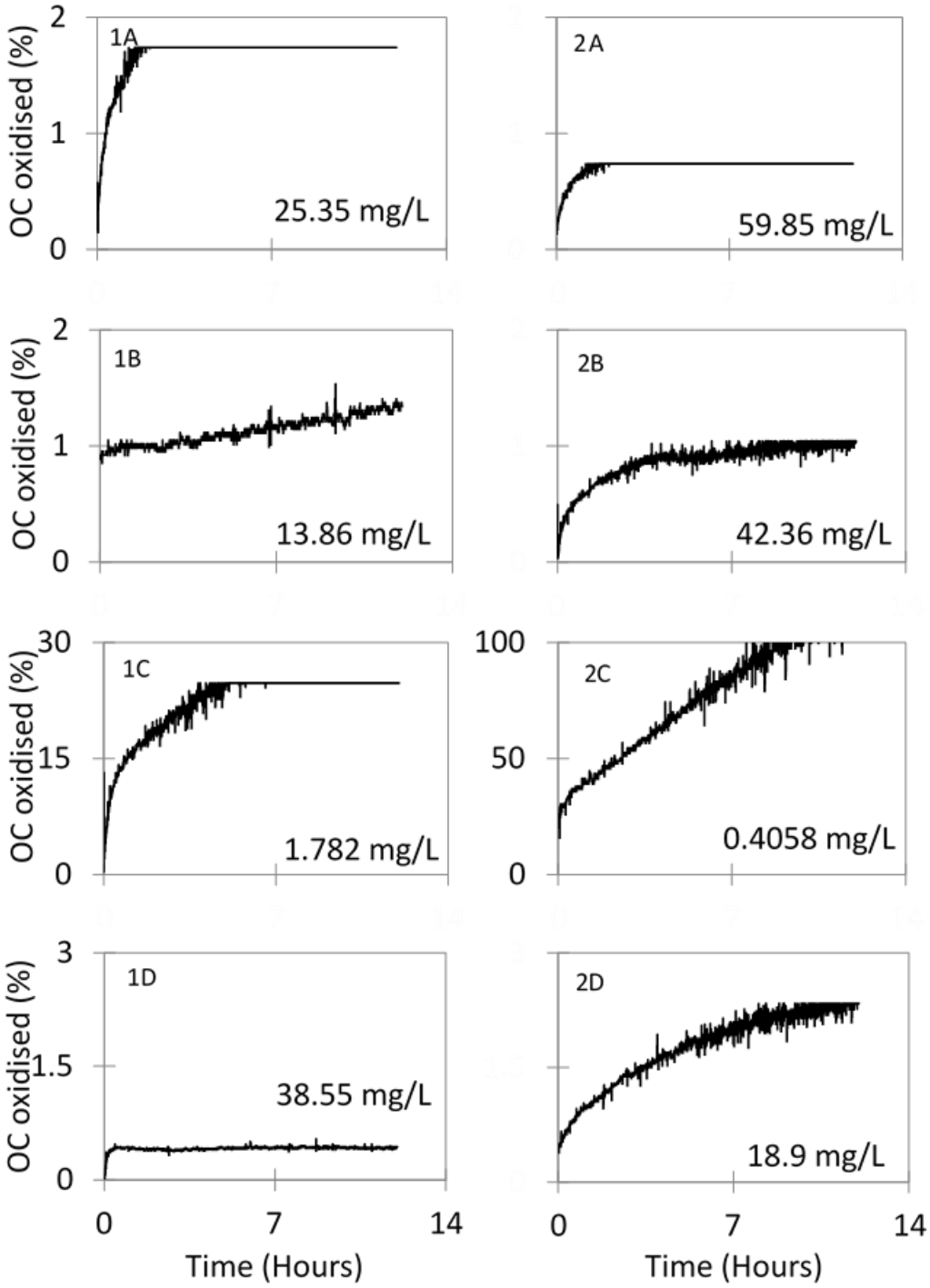

Figure 16: Percentage organic carbon oxidised over a 12-hour period of different size classifications. Numerical labelling refers to 1) Vegetated catchment 2) Eroded catchment. Alphabetic labelling refers to A) <10>3 kDa B) <10>50 kDa C) <0.2 µm> 50 kDa D) <1>0.2 µm kDa. Numbers inside graphs refer to organic carbon concentrations. Samples collected over the same event (04/04/2019).

3.4 Inorganic carbon concentrations

Mean carbon dioxide concentrations in the vegetated catchment were considerably higher than the eroded catchment, 945 ppm and 614 ppm, respectively (Fig. 17 1A and 2A). In both catchments strong diurnal variability was observed for all three parameters (Fig. 17 A, B and C). For the vegetated catchment mean stream temperature and pH were 11.35 ^{o}C and 6.26, respectively. In comparison, for the eroded catchment mean values were 9.97 ^{o}C and 6.07, respectively. For both catchments, higher carbon dioxides concentrations were observed at low-flow and during an event they decreased considerably (Fig. 17 1A and 2A). A larger decrease was observed at the eroded catchment with concentrations dipping below atmospheric concentrations (352.82 ppm) (Fig. 17 2A). Post-event concentrations are quickly recharged in both catchments, especially evident at the eroded catchment in which concentrations become highly saturated reaching 822.15 ppm (Fig. 17 2A).

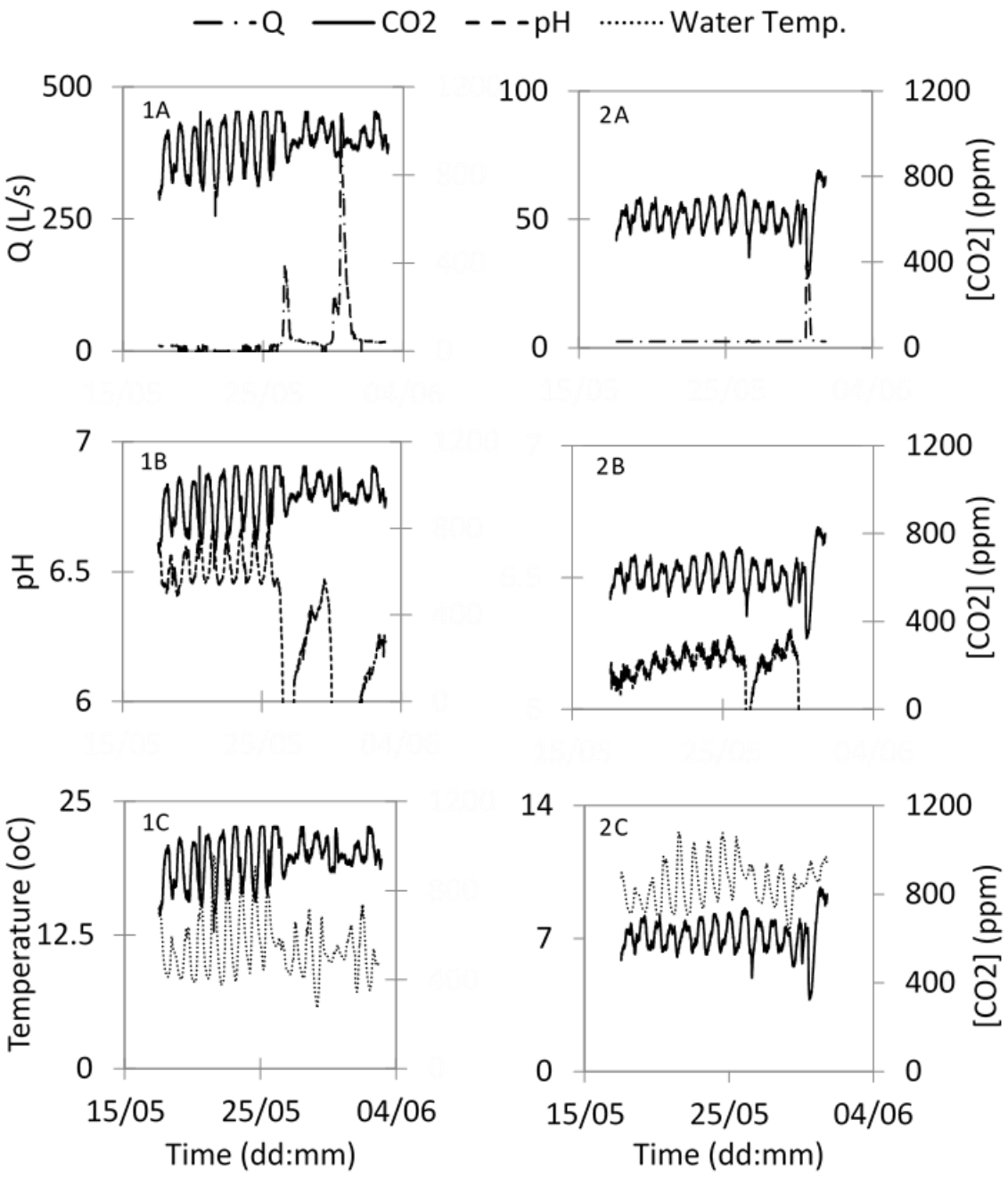

Figure 17: Time series plots of CO2 concentrations (ppm) against three different parameters; discharge (L/s), pH and in-stream temperature (°C) between 17/05/2019 to 03/05/2019. Numerical labelling refers 1) Vegetated catchment 2) Eroded catchment. Alphabetic labelling refers A) Discharge B) pH C) Temperature.

4.0 Discussion

4.1 Rating relationship of vegetated and eroded catchments

Rating relationships used to calculate fluxes at both catchments were generally poor with high amounts of scatter (Fig. 3 & 4), showing the errors that can arise from estimations calculated via extrapolation, although, a number of the relationships were significant.

In the eroded catchment event rating relationships, the >0.2 µm rating (r^2 = 0.38) had greater scatter than the vegetated site (r^2 = 0.42). Unexpected, as previous literature has suggested that particulate organic matter at eroded catchments should have a strong relationship with discharge as surface run-off will mobilise large peat material rather than small material (Pawson, et al., 2008; Pawson, et al., 2012). The eroded catchment <0.2 µm relationship was relatively weak (r^2 = 0.44) but significant (p >0.05). This is in disagreement with findings in Pawson et al. (2008), in which a very weak relationship between discharge and dissolved organic carbon concentrations (r^2 = 0.15) was observed at an eroded catchment. The eroded catchment <0.2 µm event rating relationship also had a much stronger relationship (r^2 = 0.44) than the corresponding vegetative catchment rating (r^2 = 0.0404). Only the <0.2 µm at the vegetated catchment was not significant (p >0.05) in all the event rating relationships. In warming climatic scenario, evidence from event rating relationships suggest a higher flux of smaller material to be exported during high-flow events.

The vegetated catchment baseflow rating relationships, both size fractions had negative slopes, although, the >0.2 µm fraction was not significant (p >0.05). This suggests small discharge increases are causing dilution of the organic carbon present. The eroded site baseflow ratings of the two >0.2 µm fractions had a negative relationship. Although the <0.2 µm fraction actually had a positive relationship contrasting to the vegetative site. Only the <0.2 µm rating of the <50 L/s range was significant (p < 0.05). A positive relationship implies a minimal increase in run-off is required to dislodge small material, although, relationships were very weak (r^2 <0.1). The subjective term for “baseflow” is a potential explanation for the weak relationships observed. Baseflow can vary yearly/seasonally depending on a number of

factors e.g. volume of rainfall or volume of water required to mobilise material. This means that an event one year could be perceived as baseflow the next year or visa versa.

4.2 Inference of organic carbon flux from hydrology and water chemistry

In this study, the vegetated catchment is used as a control as it has not been subject to any profound change. Firstly, to see if there are differences between the two catchments. Secondly, if any alteration can be observed post-restoration at the eroded catchment. There are clear differences in the catchments that make for difficult comparisons i.e. size, volume of rain received (Fig. 5) and topography. Comparison of the duration at which the rain fell at the two catchments can provide a degree of similarity. If rain fell over the same period of time; it is inferred that the two catchments should have experienced it in similar ways. This is observed in (Fig. 5 1A and 2A). In addition, there is minimal literature that consider the response of streamflow to revegetation restoration practises.

Hydrological flow through the two catchments are clearly different observed in Fig. 5. In 2003, the discharge was higher than the baseflow 25% of the time at the vegetated catchment compared to 12% at the eroded catchment. This difference could indicate a “flashier” response to rainfall at the eroded catchment, which can be attributed to the increase in velocity of surface run-off on the basis of vegetation reduction (Holden, et al., 2008; Parry, et al., 2014). In 2018, conditions were very contrasting with a considerable reduction in rainfall. Surprisingly, the eroded catchments discharge at low-flow was greater than in 2003, which is unusual if less rain has fallen. This discrepancy is presumably attributed to variations in the stage-discharge curves used for the two different years (See supporting information (Fig. S3)).

Run-off coefficients suggests that a higher proportion of rain was being converted to discharge at the eroded catchment in post-restoration years. Indicating further degradation of conditions, although, relative response to restoration can be attributed to “individualism” of a site. It is possible for conditions to get seemingly worse or recover slowly. It was also difficult to establish whether any significant change has occurred when analysing only three months

that meteorologically were so contrasting which indicates that higher resolution data must be analysed to gain a better understanding of conditions at the two catchments.

Analysis of individual events may provide greater evidence of disparity between the two catchments and changes relative to restoration. Aside from the two abnormal events, the run-off coefficients presented in Fig. 6 provide evidence that the catchments are relatively similar prior to and during the restoration. Contrary to expectations, higher run-off coefficients are observed at the vegetated catchment. Further evidence was provided in the cumulative rain and discharge plots, suggesting a greater response of discharge to rain, especially evident in the 2003 event (Fig. 8 1B). This indicates a higher proportion of rainfall was converted to surface run-off and no infiltration occurred. Previous work has stated that a water table closer to the surface can increase the volume of surface run-off (Holden, et al., 2004; Katimon, et al., 2013). It would explain why at times that the eroded catchment has seemingly a greater water retention capacity, as eroded catchments are known to have consistently lower water tables (Holden, et al., 2004; Katimon, et al., 2013; Martin-Ortega, et al., 2014). However, this should only be evident in a few events, as erosion produces gullies in the peat, which provides a direct path for water flow (Evans, et al., 2006; Martin-Ortega, et al., 2014; Shuttleworth, et al., 2019). Another plausible explanation is the unreliability of the eroded catchment stage-discharge curves.

Time to peak values (Fig. 7B) may provide a further insight of the disparity between the two catchments. As the two abnormal events are not observed to have a faster time to peak, it suggests that even though there may be a greater volume of run-off, it was sufficiently retarded by surface vegetation. Furthermore, time to peak doesn't rely on an error-prone conversion from stage to discharge, only the time in which the increase occurs is considered. Average time to peak in events for the eroded catchment were one hour faster, indicating that run-off was moving overland and entering the stream much quicker. Evidence provided by the time to peak, in reference to an organic flux, indicates the eroded catchment should have a higher carbon flux prior to the restoration.

In 2019, conditions have seemingly improved at the eroded catchment. Run-off coefficients greatly decrease (Fig. 7A) and time to peak increases. Higher vegetation cover on the peat surface could be attributed to improvements as greater retardation of surface run-off would slow input in to stream and allow greater time for infiltration (Holden, et al., 2008). Although, since the increase in time to peak was observed at both catchments, it may be a result of the characteristics of the rainfall event. Based on the evidence, there was some indication that the restoration project has improved hydrological conditions. Inferring, from a hydrological view, that the two catchments should have similar carbon fluxes in 2019

Damaged peatlands can lead to greater acidity in streamflow. In both Jones (2004) and Clark et al. (2008) a lowering water table caused aeration in peat leading to sulphuric acid formation. Subsequently, surface water from rainfall can mobilise sulphuric acid, entering the stream. The eroded catchment should therefore have a lower pH stream measurement. In 2003, results show that difference in pH between the two catchments are not considerably different (Fig. 9). Prior to restoration, the only major difference arises from the alkaline range of pH, which suggests slightly more acidic conditions at the eroded catchment. In 2019, both catchments demonstrate greater acidity which can imply a greater volume of water moving through the system or worsening conditions. At the vegetative catchment, a larger volume of water was observed than in 2003 which can be attributed to greater rainfall. However, at the eroded catchment a lower volume of water was transported compared to 2003. Unfortunately, no rainfall data was available in May, June and July 2019 to confirm this. A study on ditch blocking restoration observed that a rising water table had led to a decrease in stream water pH (Wilson, et al., 2011), which could have attributed to the lower pH in 2019 at the eroded catchment. Although, as stated the high discharge at the vegetated catchment would infer a higher volume of rainfall, thus, discharge at both catchments should be higher. Another explanation for the difference is the weakness of the stage-discharge curve used in this study. Variability between the years could be attributed to the different calibration curves used to convert pH from the raw sensor measurement (See supporting information - Fig. S4 & Fig. S5,

2003 calibration not available). A reduction of percentage time of pH <5 in stream was also observed in 2019 compared to 2003 in both catchments, further complicating the difference between the years. In relation to the organic carbon flux, results suggest that conditions should be similar in the two catchments.

As with the hydrological comparisons, analyses of individual events will provide higher resolution (Fig. 11). In 2003, time to peak was on average faster by an hour at the eroded catchment but unlike hydrology, a significant decrease isn't observed in 2019 during the same event. A suggestion that pH could be controlled by other environmental processes than just hydrological flow regimes e.g. acidity of rain. Thus, observation of the H^+ flux response to discharge and rain input may provide greater resolution for explanation on the processes occurring.

In 2003, at the vegetated catchment, stream H^+ increases prior to discharge (Fig. 11), suggesting that stream H^+ flux can be responsive to rain acidity. Although, observation of the disparity in magnitudes of H^+ entering the system and H^+ in-stream would be contradictory of this. In the same year, the eroded site stream H^+ concentrations are much more responsive to discharge. This result provides evidence that run-off has a much shorter residence time and less contact with weathered alkaline mineral surfaces, a suggested source of acidity to stream water (Jones, 2004). Unexpectedly, H^+ concentrations are higher at the vegetated catchment, and the lower degree of infiltration would suggest a higher H^+ concentration at the eroded catchment. In 2019, the vegetated catchment has a greater response to discharge than 2003. Surface run-off is the most plausible source of acidity, contradictory to 2003. In contrast, the eroded catchment exhibits a strange disconnection between pH and discharge. The stage-discharge curve can be attributed to this rather than “real” data further exploiting its weakness. It was a lot more difficult to infer the carbon flux from water chemistry comparisons owing to the low number of events. Although, with a faster time to peak in 2003 it would be assumed that the flux prior to restoration would be larger. Post-restoration from pH data shows that no decrease should be observed, and that the flux will likely be similar.

This study acknowledges that the number of events analysed was low. A greater number is required in order to fully understand the eroded catchment response to the restoration project. Inference of the flux change was made even more difficult as an area of damaged peat remains at the eroded catchment. However, this was not a study on the success of a restoration project, these observations have been made to infer whether the organic carbon flux has changed. So, observations made here will be taken as interpreted. From hydrological comparisons and water chemistry analysis, the flux would be expected to be larger at the eroded catchment in years preceding and during the restoration (2007 to 2010); although, there was some discrepancy in the water chemistry results. Post-restoration, there should be a decline in flux as hydrological conditions have seemingly improved. Although no evidence was provided from water chemistry to suggests this, interpretation was based on hydrological response.

4.3 Inter-comparison of current & previous flux estimations

Fluxes calculated in Jackson (2010) and Phai (2012), are contradictory to values found in the present study and inference from hydrological & fluvial chemistry characteristics (Fig. 13). Fluxes are significantly lower, with the exception of 2008, and exhibit a contrasting result as the vegetated catchment was greater than the eroded catchment every year. This is contradictory of many other studies too, in which fluxes at eroded catchments are usually greater (Evans, et al., 2006; Yeloff, et al., 2006; Pawson, et al., 2008; Pawson, et al., 2012). Although, there are a number of reasons for the disparity among previous and current estimates. Table 1, shows that in Jackson (2010) between 2006 to 2009 only 31 data points were available at both catchments, a low sample size that was likely unrepresentative of the study period. Phai (2012) uses a similar number of points except in 2010, in this year a daily sampling regime was conducted and a greater number of data points were available than in 2017 to 2019. Yet, the 2010 flux was severely underestimated compared to the current study. This was likely due to the daily sampling regime, emphasizing the consequence of excluding discharge events. The 2008 flux for the vegetated catchment in both of the studies was considerably greater than all years in 2017 to 2019. Samples collected in that year, by Jackson (2010) and Phai (2012) were likely collected at higher flows than previous years and with a considerably small sample size led to overestimation. Even samples collected in this study are not representative of a full year (Fig. 12). Organic carbon concentrations are missing for winter at both catchments and summer at the vegetated catchment. Previous work has observed strong seasonal variance for organic carbon concentrations (Grieve, 1990; Dinsmore, et al., 2013), suggesting a possible underestimation of both fluxes, especially at the vegetated catchment.

4.4 Intra-comparison of current flux estimations

In 2017 to 2019 the carbon flux was always significantly higher at the eroded catchment (Fig. 13). The vegetated catchment fluxes calculated via interpolation and rating; 5.86 t km^{-2} yr^{-1} & 10.58 t km^{-2} yr^{-1}, respectively. The eroded catchments estimated by interpolation and rating methods were 36.1 t km^{-2} yr^{-1} & 21.83 t km^{-2} yr^{-1}, respectively. Fluxes stated here are the average of the three-year period. Estimations in both methods are in agreement with previous literature at vegetated and eroded catchments, observing values in the range of 2.5 to 38.82 t km^{-2} yr^{-1} and 31.00 to 92.47 t km^{-2} yr^{-1}, respectively (Hope, et al., 1997; Evans, et al., 2006; Yeloff, et al., 2006; Pawson, et al., 2008). Results suggest that erosion is an important factor in the determination of the flux magnitude. In a scenario where peatlands will be more analogous with eroded catchments, a greater organic carbon flux is likely and thus, a greater indirect carbon dioxide flux. Previous work has indicated a positive relationship between terrestrial carbon input and carbon dioxide concentrations in many boreal environments including peatlands (Jonsson, et al., 2003; Lapierre, et al., 2013).

When looking at all three methods of flux estimation (interpolation, rating and inference by hydrology and water chemistry characteristics) there are differences. As stated, from a subjective view of the hydrology and chemistry, the two catchments organic carbon flux should have a greater degree of similarity. Although rating relationships values are more similar in value than the interpolation technique. Additionally, with the estimates from previous work it was very difficult to know whether this was a relative improvement to prior years.

In Table 2, interpolation consistently overestimated the flux in relation to rating estimates over a 24-day sampling regime. If this interpolation data was scaled for a whole year it would massively overestimate the organic carbon flux, thus a large sample size over varying temporal and spatial conditions is essential to make valid predictions. The low rating relationship estimate at the vegetated catchment highlights an issue with this method. If a strong negative correlation exists in the concentration–discharge relationship. The y-equation used to convert discharge to concentrations are calculated as negatives which are assumed

to be zero as concentrations cannot be negative. The rating method was further complicated by the relationship between concentration and discharge during an event, highlighted in the organic carbon hysteresis (Fig. 14 2A and 2B). Implications of hysteresis is that a single linear line cannot be used for multiple events, as each event will have its own spatial and temporal characteristics. This helps explain the poor scatter observed in the event rating relationships as multiple events are plotted against each other (Fig. 3 & 4). Furthermore, a single linear line cannot be used for a single event, due to the rising and falling nature of organic carbon concentrations throughout an event. A solution to this would be to split up rating curves into individual sections of the event i.e. rising and falling limb, although, this requires a large amount of work especially when a large number of events can be considered. In this study, measures were completed to try and reduce this effect by splitting the rating plots into events and less than specified discharge ranges. Although, even with these improvements there are factors to consider such as the stage-discharge curve and individualism of each event that cannot be controlled. Aside from the problems with these methods, estimations found in this study were sufficient.

4.5 Temporal & spatial significance of particle size distribution

Particle size distributions vary over discharges, larger sized material was observed to increase with increasing discharge (Fig. 15A). Particle size distribution at the lowest discharge was collected by Phai (2012), which was all large material. This was likely due to Phai (2012) not having access to the two smallest cut-off plates used in this study, <10>3 kDa and <3 kDa. Although, it is possible that a high proportion of large material was present at low discharges but it would be considered highly unlikely.

Particle size distribution at the eroded catchment shows a positive relationship between larger material and discharge. At the highest discharge range, the two smallest fractions at the eroded catchment become the least dominant. Damaged peat is more susceptible to erosion by surface run-off causing a greater amount of large material to be in stream (Pawson, et al., 2008; Pawson, et al., 2012). At the vegetated catchment a positive relationship of larger material and discharge was also observed; however, the two smallest fractions maintain their dominance. There may be two reasons for this. Firstly, the higher proportion of vegetation cover anchors the peat, so throughout an event less large material is likely to enter the stream (Limpens, et al., 2008). Secondly, carbon deposited may be of autochthonous origin, which is likely to be smaller in size (Amon & Benner, 1996). Even though these fractions are in these proportions at the range of discharges observed their importance in relation to spatial-temporal variance cannot be concluded without consider their flux.

The vegetated catchment had a larger flux by ~15 t km^{-2} yr^{-1} a suggestion that the sub-micron flux will become smaller in a future when peat becomes more damaged, which is inconsistent with previous analysis which usually showed the eroded catchment to have the larger organic carbon flux. A positive relationship was observed with discharge and total flux (Fig. 15 1C and 2C). Fluxes at the eroded catchment coincide with this trend until the significant drop at >50 L/s, which could be due to a significant proportion of the flux being absent as material mobilised at high discharges would likely be particulate (Pawson, et al.,

2008; Pawson, et al., 2012). All sizes are considered here are sub-micron potentially overlooking a large proportion of the exported flux.

Fluxes calculated by this method when compared to interpolation and rating relationship calculations are higher or similar (Fig. 13A and 13B). This is highly unlikely as the flux here only considers the <1.6 µm fraction, in which there would a proportion of carbon that is larger than this. Raising concerns of unrepresentative sampling for the particle size distribution, which ranged from two to five samples and the highest number of samples collected for the lower boundaries of discharges. An additional explanation for the overestimation is the method used to interpolate the fluxes, using the sum of discharges of respective ranges in the area under the curve (Fig. 15 1B and 2B) is unrepresentative. Discharge conditions of an individual year in which the samples were collected could be contrasting to this amalgamation of all discharges.

4.6 Lability of particle size distributions

To note, the <3 kDa size fraction could not be tested in the lability experiments as no retentate was collected, it was only calculated from the mass balance calculations. As stated, the <1> 0.2 µm acted as a control and all smaller size classification should be sterile. Although, Wang et al. (2007) has shown that the passage of microbes though 0.1 µm filters is possible, which could have influenced the <0.2 µm> 50 kDa size.

Intra-comparison of fractions was made more difficult by the negative relationship between concentration and percentage of carbon oxidised, as observed in the <0.2 µm> 50 kDa fraction of both catchments (Fig. 16 1C and 2C). Lability experiment results demonstrate two things. First, the oxidative process is a significant pathway to carbon dioxide conversion. Secondly, different size fractions have varying degrees of lability in relation to size. The smallest fractions, in both catchments were the most liable (Fig. 16 1A and 2A) and the largest the least. Intra-variation did arise between the two smallest fractions, the vegetated sample was observed to be more liable. Previous work has suggested that organic carbon from autochthonous origin will have a greater degree of lability as it is easier to breakdown (Amon & Benner, 1996). Since experiments are not complete natural simulations processes in ambient waters may differ and there will likely be additional controls on organic carbon breakdown, possibly enhancing or retarding this process. Worrall et al. (2006) could not explain the rapid rate of dissolved organic carbon loss by just microbial and photochemical reactions, the oxidative pathway could aide explanation of the loss rate observed.

A significant proportion of carbon in the <10>3 kDa fraction can be converted to carbon dioxide in a relatively short time scale. There is a potential for a large carbon dioxide flux as this fraction is released in relatively large amounts by both catchments. In terms of a scenario in which a greater number of peatland systems become more analogous with the eroded catchment, fluxes of the more liable fractions will not change to a great degree and a carbon dioxide increase is not likely. Although, the <3 kDa fraction does doubles compared to the vegetated catchment but the lability of this fraction could not be tested. Based on the

relationship of liability and size, it could be a very liable fraction which suggests an increased carbon dioxide flux in a warming scenario. The lability of the particulate fraction of organic carbon was not investigated in this study, which is a large potential source of carbon dioxide.

4.7 Inorganic carbon concentration

Carbon dioxide concentrations observed in both catchments are supersaturated in respect to atmosphere which has been commonly observed in literature (e.g. Hope, et al., 2001; Billett, et al., 2004; Dawson, et al., 2004; Hope, et al., 2004; Billett, et al., 2007; Billett & Moore, 2008; Dinsmore & Billett, 2008; Dinsmore, et al., 2009; Dinsmore, et al., 2010; Dinsmore, et al., 2013).

Stream carbon dioxide concentrations, pH and temperature all showed strong diurnal variations during low-flow. Although, there is likely one parameter that controls the variation of carbon dioxide concentrations. Inorganic carbon speciation can be altered by pH dynamics, an alkaline pH is favourable to bicarbonate forming conditions and acidic pH is favourable to carbon dioxide forming conditions. However, a small range of deviation was observed for pH at the vegetated and eroded catchments (0.1-0.3 and 0.05–0.1, respectively). The strong diurnal nature of the carbon dioxide concentrations is then likely attributed to water temperature-dependent solubility, which is consistent with literature (Billett, et al., 2004; Dinsmore & Billett, 2008; Dinsmore, et al., 2013). It is likely then that carbon dioxide concentration dynamics are due to dissolved and gaseous variation, and this likely influences the pH of the stream. Consequently, carbon dioxide fluxes calculated by headspace analysis from peatland draining catchments may have been underestimated if sample collection only occurred through the day. The lower concentrations detected during the day are presumably a result of higher evasion rates from the stream surface as a higher proportion of carbon dioxide is in the gaseous form.

During a discharge event, a decrease occurs with peak discharge at both catchments which has been observed in previous literature (e.g. Hope, et al., 2001; Hope, et al., 2004; Billett, et al., 2004; Billett & Moore, 2008; Dinsmore, et al., 2010). Evasion rates of carbon dioxide are highest at these peak flows and the significant drop observed in pH (< 5) favours gaseous carbon dioxide. This confirms the requirement of high temporal resolution in carbon dioxide flux studies in peatland draining catchments

Throughout the period of measurement, carbon dioxide concentrations were, on average, greater at the vegetated catchment. Stream water carbon dioxide concentrations can be influenced by a number of terrestrial factors, i.e. plant respiration or biological activity (Dawson, et al., 2002; Billett, et al., 2004; Dawson, et al., 2004; Hope, et al., 2004). Throughout a rainfall event free gaseous carbon dioxide can be “flushed” out of the peat maintaining it above atmospheric concentrations. This is likely why the concentrations at the vegetated catchment are not diluted to the same extent as the eroded. In addition, topological features can also affect evasion rates i.e. greater stream gradient and more turbulent nature, which are more severe at the eroded catchment (Hope, et al., 2001; Billett, et al., 2007; Dinsmore, et al., 2010). Seasonal variance at the two catchments could not be considered due to data limitations. From this result, it would suggest if peatlands become damaged to a greater extent stream carbon dioxide concentration will possibly decrease. Although, will remain supersaturated in relation to the atmosphere, and “hotspots” of carbon dioxide production.

5.0 Conclusion

Hydrological and water chemistry conditions at the eroded catchment were interpreted as being improved post-restoration. Thus, the magnitude of the organic carbon flux should have decreased in the current study period. Although, there was a great deal of uncertainty in interpretation. In order to confirm the full extent of the impact of restoration a greater magnitude of information must be collected, i.e. greater number of events.

Fluxes calculated via interpolation and ratings differed greatly at both catchments; interpolation overestimating the flux in 2017 to 2019 in relation to the rating method at the eroded site and the rating overestimating the flux in relation to interpolation at the vegetated site. In comparison to the subjective inference of the flux, conditions have not improved as suggested. Quantitative comparison from previous work are difficult as fluxes in this study are significantly higher. The differences observed in this study and previous work is likely due to unrepresentative sampling. Estimates in this study could be perceived as more accurate to the “true” value. Although, there are still problems associated with the calculations in 2017 to 2019 e.g. sampling does not account for a whole year or the hysteresis of events. Thus, a high degree of error was still associated with calculations. Further work must be completed to reduce these errors such as finding a method that can provide continuous organic carbon measurements. In a warming scenario, carbon fluxes are likely to increase, increasing the potential of an indirect carbon dioxide flux. Generating a positive feedback to global warming. This was validated by the interpolation and rating relationships estimating a higher carbon flux at the eroded catchment, a model for peatlands of the future.

The sub-micron flux is not likely to change to a great degree in a global warming scenario and may even decrease; although, the <3 kDa fraction increased at the eroded catchment. There was a suggestion that the largest material will dominate the flux at very high discharges; however, unrepresentative sampling and low number of samples likely caused high errors. Further work must address this, collecting a greater number of samples and finding a more robust method of flux estimation. It was found that organic carbon oxidation is a major

pathway for carbon dioxide production. In addition, a negative relationship between size and lability was observed. A potential large indirect carbon dioxide can be produced from these smaller fractions as they are dominant in terms of flux at both catchments. It is suggested that work is built upon this further as not all organic carbon sizes were investigated such as the particulate fraction, a large potential source of indirect carbon dioxide. Also, inoculants of unfiltered water samples should be added to size fractions to further test the significance of the oxidative pathway vs microbial and produce more natural simulations.

Inorganic carbon fluxes were shown to be higher during low-flow and controlled by diurnal temperature variations. During periods of high-flow, concentrations decreased at both catchments; this was more apparent at the eroded catchment. In a warming scenario, free carbon dioxide concentrations will possibly decrease as biological activity and soil respiration will reduce with a greater degree of erosion. Although, much more continuous measurements must be collected in order to account for seasonal variance. In order to make a more accurate prediction of how these areas will be affected by climate change, a full carbon budget study has to be conducted on an eroded peat catchment. To the author's knowledge, none have been completed so far.

An underlying issue for all calculations and comparisons was the stage-discharge curve. Unreliability of this is a fundamental source of error. The method of gauging on site is clearly insufficient for capturing extreme spatial-temporal variability. Further work must address this issue in order to reduce error and improve the accuracy of prediction. A possible method to investigate would be a remote gauging method that would be triggered during an event.

Bibliography

Amon, R. M. & Benner, R., 1996. Photochemical and microbial consumption of dissolved organic carbon and dissolved oxygen in the Amazon River system. *Geochimica et Cosmochimica Acta,* 60(10), pp. 1783-1792.

Billett, M. F., Garnett, M. H. & Harvey, F., 2007. UK peatland streams release old carbon dioxide to the atmosphere and young dissolved organic carbon to rivers. *Geophysical Research Letters,* Volume 34, p. doi:10.1029/2007GL031797.

Billett, M. F. & Moore, T. R., 2008. Supersaturation and evasion of CO2 and CH4 in surface waters at Mer Bleue peatland, Canada. *Hydrological Proccesses,* 22(12), pp. 2044-2054.

Billett, M. F. et al., 2004. Linking land-atmosphere-stream carbon fluxes in a lowland peatland system. *Global Biogeochemical Cycles,* 18(1), p. 10.1029/2003GB002058.

Brown, S. L., Gouslbra, C. S. & Evans, M. G., 2018. Controls on fluvial carbon efflux from eroding peatland catchments. *Hyrdological Processes ,* 33(9), pp. 361-371.

Butman, D. & Raymond, P. A., 2011. Significant efflux of carbon dioxide from streams and rivers in the United States. *Nature Geoscience ,* Volume 4, p. 839–842.

Charman, D., 2002. *Peatlands and environmental change..* Chicester : John Wiley & Sons Ltd.

Clark, J. M., Lane, S. N., Chapman, P. J. & Adamson, J. K., 2008. Link between DOC in near surface peat and stream water in an upland catchment. *Science of the Total Environment ,* 404(2-3), pp. 308-315.

Dawson, J. J. C. et al., 2004. Sources and sinks of aquatic carbon in a peatland stream continuum. *Biogeochemistry,* 70(1), p. 71–92.

Dawson, J. J. C., Billett, M. F., Neal, C. & Hill, S., 2002. A comparison of particulate, dissolved and gaseous carbon in two contrasting upland streams in the UK. *Journal of Hydology ,* 274(1-4), pp. 226-246.

Dinsmore, K. et al., 2010. Role of the aquatic pathway in the carbon and greenhouse gas budgets of a peatland catchment. *Global Change Biology ,* p. 2750–2762.

Dinsmore, K. J. & Billett, M. F., 2008. Continuous measurement and modeling of CO2 losses from a peatland stream during stormflow events. *Water Resources Research,* Volume 44, p. doi:10.1029/2008WR007284.

Dinsmore, K. J., Billett, M. F. & Dyson, K. E., 2013. Temperature and precipitation drive temporal variability in aquatic carbon and GHG concentrations and fluxes in a peatland catchment. *Global Change Biology ,* 19 (7), pp. 2133-2148.

Dinsmore, K. J., Billett, M. F. & Moore, T. R., 2009. Transfer of carbon dioxide and methane through thesoil-water-atmosphere system at Mer Bleue peatland, Canada. *Hydrological Processes,* Volume 23, p. 330–341.

Evans, M., Warburton, J. & Yang, J., 2006. Eroding blanket peat catchments: Global and local implications of upland organic sediment budgets. *Geomorphology,* pp. 45-47.

Evans, M., Warburton, J. & Yang, J., 2006. Eroding blanket peat catchments: Global and local implications of upland organic sediment budgets. *Geomorphology ,* 75(1), pp. 45-57.

Everett, C. R., Chin, Y.-P. & Aiken, G. R., 1999. High-pressure size exclusion chromatography analysis of dissolved organic matter isolated by tangential-flow ultrafiltration. *Limnography and Oceanography ,* 44(5), pp. 1316-1322.

Fenner, N. & Freeman, C., 2011. Drought-induced carbon loss in peatlands. *Nature Geoscience ,* 4(11), pp. 895-900.

Gaffney, J. W., White, K. N. & Boult, S., 2008. Oxidation State and Size of Fe Controlled by Organic Matter in Natural Waters. *Environmental Science and Technology ,* 42(10), p. 3575–3581.

Grieve, I. C., 1990. Seasonal, hydrological, and land management factors controlling dissolved organic carbon concentrations in the loch fleet catchments, Southwest Scotland. *Hydrological Processes ,* 4(3), pp. 231-239.

Holden, J., Chapman, P. & Labad, J., 2004. Artificial drainage of peatlands: hydrological and hydrochemical process and wetland restoration. *Progress in Physical Geogrpahy: Earth and Environment,* 28(1), p. 95–123.

Holden, J. et al., 2008. Overland flow velocity and roughness properties in peatlands. *Water Resource Research ,* Volume 44, pp. W06415, doi:10.1029/2007WR006052.

Holden, J. et al., 2007. Environmental change in moorland landscapes. *Earth Science Reviews ,* 82(1-2), pp. 75-100.

Hope, D., Billet, M. F., Miln, R. & Brown, T. A. W., 1997. Exports of Organic Carbon in British Rivers. *Hydrological Processes ,* Volume 11, p. 25±344 .

Hope, D., Palmer, S. M., Billett, M. F. & Dawson, J. J. C., 2001. Carbon dioxide and methane evasion from a temperate peatland stream. *Limnology and Oceanography ,* 46(4), pp. 847-857.

Hope, D., Palmer, S. M., Billett, M. F. & Dawson, J. J. C., 2004. Variations in dissolved CO2 and CH4 in a first-order stream and catchment: an investigation of soil–stream linkages. *Hydrological Processes,* 18(17), pp. 3255-3275.

Ise, T., Dunn, A., Wofsy, S. & Moorcroft, P., 2011. High sensitivity of peat decomposition to climate change through water-table feedback. *Nature Geosciences ,* 1(11), pp. 763-766.

Jackson, A., 2010. Monitoring and determining controls on fluxes of natural organic matter. *In: Faculty of Engineering and Phisical Sciences, Degree of PhD. The University of Manchester.*

Jackson, A., Gaffney, J. W. & Boult, S., 2012. Subsurface Interactions of Fe(II) with Humic Acid or Landfill Leachate Do Not Control Subsequent Iron(III) (Hydr)oxide Production at the Surface. *Environmental Science and Technology ,* 46(1), p. 7543–7550.

Johnson, M. S. et al., 2010. Direct and continuous measurement of dissolved carbondioxide in freshwater aquatic systems—methodand applications. *Ecohydrology ,* Volume 3, p. 68–78.

Johnson, M. S. et al., 2008. CO2 efflux from Amazonian headwater streams represents a significant fate for deep soil respiration. *Geophysical Research Letters,* Volume 35, p. doi:10.1029/2008GL034619.

Jones, J. A. A., 2004. Implications of natural soil piping for basin management in upland Britain. *Land Degredation & Development ,* 15(3), pp. 325-349.

Jones, T. G. et al., 2016. Transformations in DOC along a source to sea continuum; impacts of photo-degradation, biological processes and mixing. *Aquatic Sciences ,* 78(3), pp. 433-446. DOI: 10.1007/s00027-015-0461-0.

Jonsson, A., Karlsson, J. & Jansson, M., 2003. Sources of Carbon Dioxide Supersaturation in Clearwater and Humic Lakes in Northern Sweden. *Ecosystems,* 6(3), p. 224–235.

Katimon, A., Shahid, S., Wahab, A. K. A. & Hazrat, M., 2013. Hydrological behaviour of a drained agricultural peat catchment in the tropics. 1: Rainfall, runoff. *Hydrological Sciences Journal,* 58(6), pp. 1297-1309.

Lapierre, J.-F. & Giorgio, P. A. d., 2014. Partial coupling and differential regulation of biologically and photochemically labile dissolved organic carbon across boreal aquatic networks. *Biogeosciences,* Volume 11 , p. 5969–5985.

Lapierre, J.-F., Guillemette, F., Berggren, M. & Giorgio, P. A. d., 2013. Increases in terrestrially derived carbon stimulate organic carbon processing and CO2 emissions in boreal aquatic ecosystems. *Nature Communications ,* Volume 4, p. Article Number: 2972.

Limpens, J. et al., 2008. Peatlands and the carbon cycle: from local processes to global implications — a synthesis. *Biogeosciences,* p. 1475–1491.

Lliguin, D. A., 2017. *Improving Characterisation of Natural Organic Matter using High Resolution Techniques in Peat Catchments, Masters of Science Thesis ,* Budapest: Central European University .

Long, H. et al., 2015. Hydraulics are a first-order control on CO2 efflux from fluvial systems. *Journal of Geophysical Research: Biogeosciences,* Volume 120, pp. 1912–1922, doi:10.1002/2015JG002955..

Maizel, A. & Remucal, C., 2017. Molecular Composition and Photochemical Reactivity of Size-Fractionated Dissolved Organic Matter. *Environmental Science & Technology ,* 51(4), pp. 2113-2123.

Mann, P. J. et al., 2012. Controls on the composition and lability of dissolved organic matter in Siberia's Kolyma River basin. *JGR Biogeoscienes ,* Volume 117, p. doi:10.1029/2011JG001798.

Martin-Ortega, J., Allott, T. E. H., Glenk, K. & Schaafsma, M., 2014. Valuing water quality improvements from peatland restoration: Evidence and challenges. *Ecosystem Services ,* Volume 9, pp. 34-43.

Mayorga, E. et al., 2005. Young organic matter as a source of carbon dioxide outgassing from Amazonian rivers.. *Nature,* Volume 436, pp. 538-41.

Miller, W. L. & Zepp, R. G., 1995. Photochemical production of dissolved inorganic carbon from terrestrial organic matter: Significance to the oceanic organic carbon cycle. *Geophysical Research Letters,* 22(4), pp. 417-420.

Montagnes, D. J. et al., 2008. Short-term temperature change may impact freshwater carbon flux: a microbial perspective. *Global Change Biology,* Volume 14, pp. 2823–2838, doi: 10.1111/j.1365-2486.2008.01700.x.

Moody, C. S., Worrall, F., Evans, C. D. & Jones, T. G., 2013. The rate of loss of dissolved organic carbon (DOC) through a catchment. *Journal of Hydrology ,* Volume 492, pp. 139-150.

Nebbioso, A. & Piccolo, A., 2013. Molecular characterization of dissolved organic matter (DOM): a critical review. *Analytical and Bioanalytical Chemistry Vol.405,* p. 109–124.

Palmer, S. M. et al., 2001. Sources of organic and inorganic carbon in a headwater stream: Evidence from carbon isotope studies. *Biogeochemistry ,* 52(3), p. 321–338.

Parry, L. E., Holden, J. & Chapman, P. J., 2014. Restoration of blanket peatlands. *Journal of Enivronmental Management,* Volume 133, pp. 193-205.

Parry, L. E., Holden, J. & Chapman, P. J., 2014. Restoration of blanket peatlands.. *Journal of Environmental Management,* Issue 133, pp. 193-205.

Pawson, R., Lord, D., Evans, M. & Allott, T., 2008. Fluvial organic carbon flux from an eroding peatland catchment, southern Pennines, UK. *Hydrology and Earth System Sciences,* 12(2), pp. 625-634.

Pawson, R. R., Evans, M. G. & Allott, T. E. H. A., 2012. Fluvial carbon flux from headwater peatland streams: significance of particulate carbon flux. *Earth Surface: Processes and Landforms ,* 37(11), pp. 1203-1212.

Phai, D. D., 2012. Quantifying organic carbon fluxes from. *In: a thesis submitted to the University of Manchester for the degree of PhD in the Faculty.*

Pickard, A. E., Heal, K. V., McLeod, A. R. & Dinsmore, K. J., 2017. Temporal changes in photoreactivity of dissolved organic carbon and implications for aquatic carbon fluxes from peatlands. *Biogeoscienes,* Volume 14, p. 1793–1809.

Shuttleworth, E. L. et al., 2019. Restoration of blanket peat moorland delays stormflow from hillslopes and reduces peak discharge. *Journal of Hydrology X,* Volume 2, p. 100006.

Sillanpää, M., Matilainen, A. & Lahtinen, T., 2014. Chapter 2 – Characterization of NOM. In: *Natural Organic Matter in Water - Characterization and Treatment Methods.* s.l.:Butterworth-Heinemann, p. 17–53.

Stimson, A. G., Allott, T. E., Boult, S. & Evans, M. G., 2017. Fluvial organic carbon composition and concentration variability within a peatland catchment—Implications for carbon cycling and water treatment. *Hydrological Processes ,* 31(23), pp. 4183-4194.

Stimson, A. G., Allott, T. E. H., Boult, S. & Evans, M. G., 2017. Reservoirs as hotspots of fluvial carbon cycling in peatland catchments. *Science of the Total Environment ,* Volume 580, pp. 398-411.

Walling, D. & Webb, B., 1981. The reliability of suspended sediment load data. Erosion and Sediment Transport Measurement. *nternational Association of Hydrological Sciences Publication,* Volume 133, pp. 177-194.

Walling, D. & Webb, B., 1985. Estimating the discharge of contaminants to coastal waters by rivers: Some cautionary comments. *Marine Pollution Bulletin,* 16(12), pp. 488-492.

Wallin, M. B. et al., 2012. Evasion of CO2 from streams – The dominant component of the carbon export through the aquatic conduit in a boreal landscape. *Global Change Biology ,* 19(3), pp. 785-797.

Wang, Y. y., Hammes, F., Boon, N. & Egli, T., 2007. Quantification of the Filterability of Freshwater Bacteria through 0.45, 0.22, and 0.1 µm Pore Size Filters and Shape-Dependent Enrichment of Filterable Bacterial Communities. *Environmental Science & Technology ,* 41(20), pp. 7080-7086.

Weiss, R., 1974. Carbon dioxide in water and seawater: the solubility of a non-ideal gas. *Marine Chemistry,* 2(3), pp. 203-215.

Weltzin, J. F. et al., 2003. Potential effects of warming and drying on peatland plant community composition.. *Global Change Biology ,* Volume 9, pp. 141-151.

Wilson, L. et al., 2011. Ditch blocking, water chemistry and organic carbon flux: Evidence that blanket bog restoration reduces erosion and fluvial carbon loss. *Science of the Total Environment,* 409(11), pp. 2010-2018.

Worral, F., Burt, T. & Shedden, R., 2003. Long term records of riverine dissolved organic matter.. *Biogeochemstry,* Volume 64, pp. 165-178.

Worrall, F., Burt, T. & Adamson, J., 2004. Can climate change explain increases in DOC flux from upland peat catchments?. *Science of the Total Environment ,* 326(1-3), pp. 95-112 .

Worrall, F., Burt, T. P. & Adamson, J., 2006. The rate of and controls upon DOC loss in a peat catchment. *Journal of Hydrology ,* 321(1-4), pp. 311-325.

Worrall, F., Howden, N. J. K. & Burt, T. P., 2013. Assessment of sample frequency bias and precision in fluvial flux calculations – An improved low bias estimation method. *Journal of Hydrology ,* Volume 503, pp. 101-110.

Yeloff, D., Labadz, J. & Hunt, C., 2006. Causes of degradation and erosion of a blanket mire in the southern Pennines. *Mires and Peat.*

6.0 Supporting information

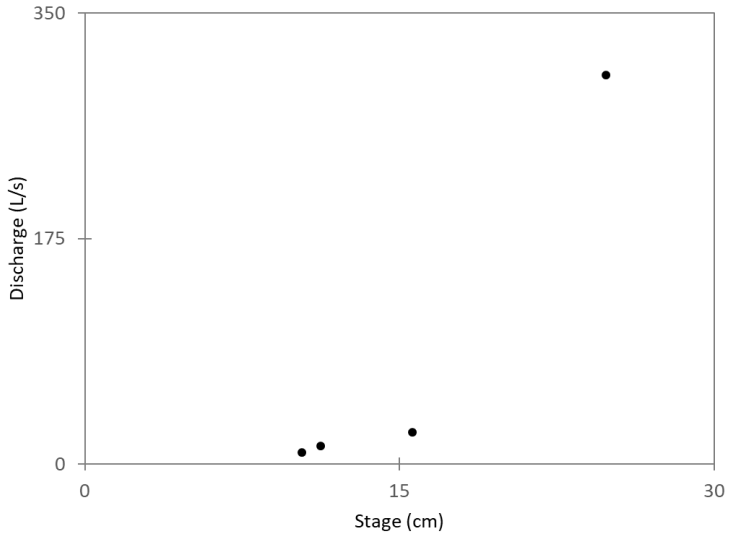

Figure S 1: Vegetated catchment stage–discharge curve (2017 to 2019)

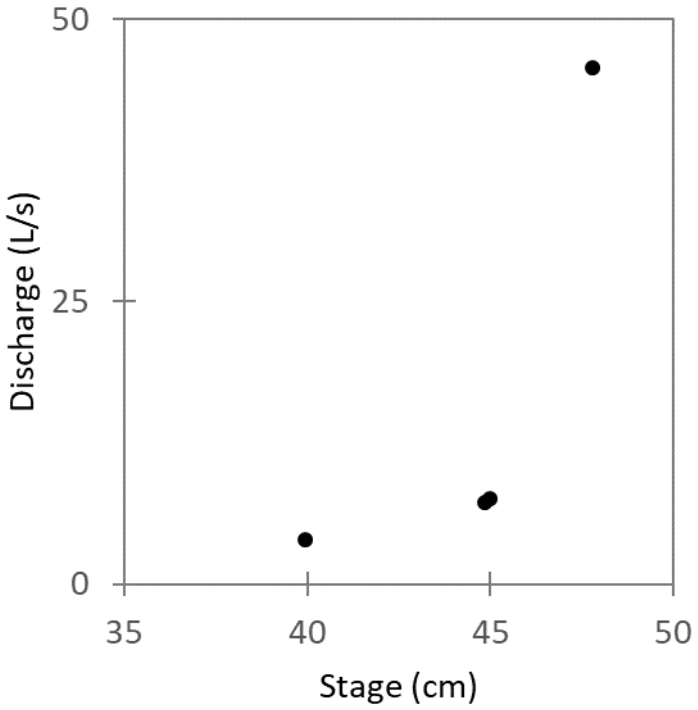

Figure S 2: Eroded catchment stage–discharge curve (2017)

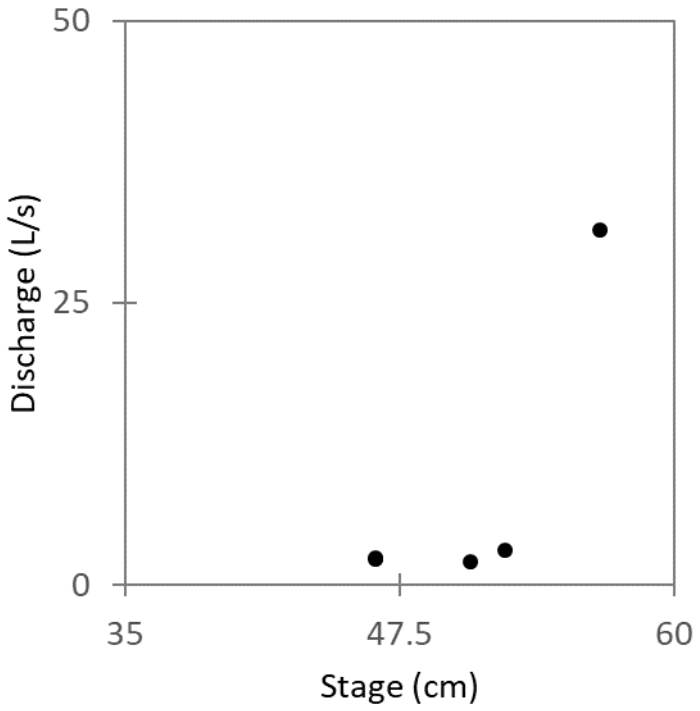

Figure S 3: Eroded catchment stage-discharge curved (2018 to 2019)

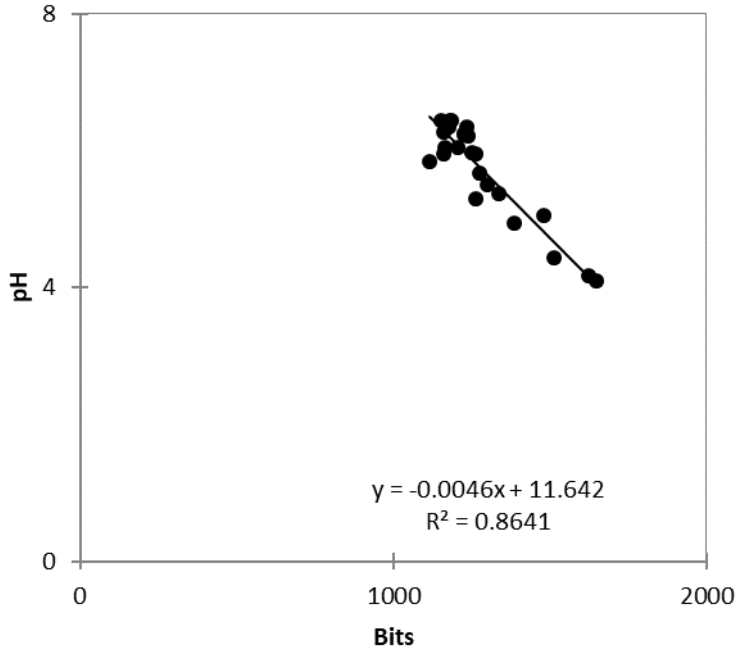

Figure S 4: Vegetated catchment pH calibration (2019)

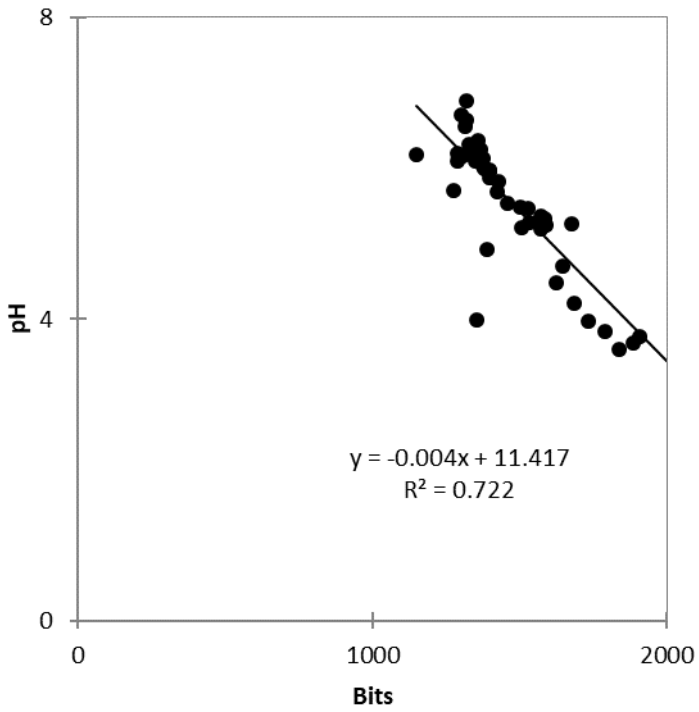

Figure S 5: Eroded catchment pH calibration (2019)